

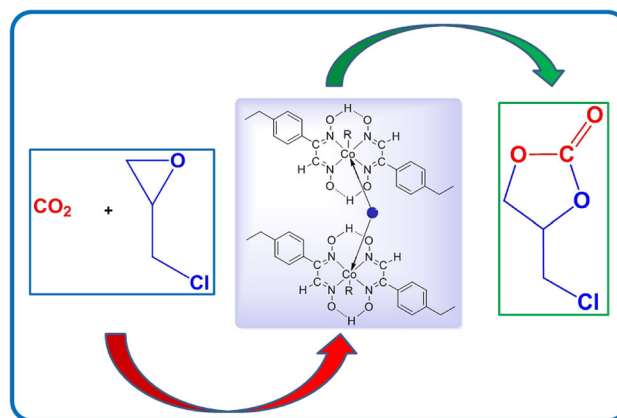
Dicobaloxime/organodicobaloximes bridged by different axial groups: synthesis, characterization, spectroscopy, and catalysis

Ahmet Kilic¹ · Hamza Fırat¹ · Emine Aytar¹ · Mustafa Durgun¹ · Aysegül Kutluay Baytak¹ · Mehmet Aslanoglu¹ · Mahmut Ulusoy¹

Received: 14 July 2016 / Accepted: 23 March 2017
© Institute of Chemistry, Slovak Academy of Sciences 2017

Abstract In this study, the various ligands axially coordinated to two cobalt center bound to the N₄-oxime core in 12 new dicobaloxime/organodicobaloxime (1–12) complexes have been synthesized and characterized by NMR (¹H and ¹³C), UV–Visible, FT-IR, LC–MS, molar conductivity analysis, melting point, and magnetic susceptibility experiments with elemental analysis. These spectroscopic results indicate that the formation of new dicobaloxime/organodicobaloxime (1–12) complexes. The (C=N–OH) peaks disappeared in the ¹H-NMR spectrum of dicobaloxime/organodicobaloxime (1–12) complexes, while new peaks were observed at range 20.18–18.33 ppm, indicating that the groups of ligands have been transformed to intramolecular H-bridge (O–H···O). The dicobaloxime (1–6) species give a better cyclic voltammogram as compared to its organodicobaloxime derivatives (7–12) due to cyclic voltammograms of the organodicobaloximes (7–12) were poor. This is possibly due to the enhanced σ donation by R groups in the organocobaloximes which are substantially stabilized. The organodicobaloxime (10) showed much better catalytic activity compared to the other cobaloxime complexes.

Graphical Abstract The different dicobaloxime (1–6) and organodicobaloximes (7–12) have been synthesized for the first time. Their redox properties were investigated using cyclic voltammetric (CV) techniques in a DMSO solution. These dicobaloximes/organodicobaloximes have been used as homogeneous catalyst for synthesis of cyclic carbonates presence of DMAP as co-catalyst.



Keywords Co(III) complexes · Dicobaloxime · Organodicobaloxime · Cyclic voltammetry · Cyclic carbonates · CO₂ fixation · Reaction parameters

Introduction

As inspired by models of Vit B₁₂ co-enzyme in various metabolisms, the different structures of cobaloxime or organocobaloximes have been synthesized (Nayak et al. 2003; Schrauzer and Kohnle 1964; Cini et al. 1998; Stolzenberg et al. 2007; Lawrence et al. 2016) and used in various field by scientists due to great interest in

✉ Ahmet Kilic
kilica63@harran.edu.tr; kilica63@hotmail.com

¹ Department of Chemistry, Faculty of Arts and Sciences, Harran University, 63190 Şanlıurfa, Turkey

coordination chemistry and broad-scope potential applications as homogeneous catalysts in synthetic chemistry reaction (Xiang et al. 2015; Yilmaz et al. 2008; Razavet et al. 2005; Du et al. 2008; Kilic et al. 2015) in polymer chemistry (Roberts et al. 2000), in liquid crystal behavior (Alici and Karatas 2016), in EPR and DFT studies (Tiede et al. 2012) and as other many areas. Besides, the cobaloxime molecules made of earth-abundant, easy-to-handle and inexpensive elements (e.g. Co elements) as homogeneous catalysts are of great potential and practical significance for artificial photosynthesis and the effective conversion of CO₂ into valuable compounds under suitable conditions, because of their earth-abundant resources, an alternate to the scarce, designable geometry, and regulatable electrochemical properties (Wang et al. 2015; Kilic et al. 2013a; 2014). Up to now, the literature research shows that numerous mononuclear Co(III) cobaloximes have been synthesized and described, whereas reports on the structure of Co(III) dicobaloximes examples are rather rare (Brown 1972; Herlinger and Ramakrishna 1985; Randaccio 1999; Dreos et al. 2010). Most of the homoaxial or heteroaxial ligand bridged dicobaloxime complexes reported to date contains pyrazine or similar groups as the bridging ligand (Dutta et al. 2015; Kumar and Seidel 2013). However, research on the structure of the chloro or benzyl groups and neutral diamine containing bridged dicobaloxime/organodicobaloxime complexes is rather rare.

A number of studied catalytic systems containing equivalent homoaxial or non-equivalent heteroaxial bridging ligands have been shown to affect the geometry of the complex and redox properties of the Co(III) center of cobaloximes (Serroni et al. 1996). From recent reports, different design of cobaloxime or cobalt oxime catalysts that have been utilized in electrocatalytic and photocatalytic water splitting have been described in detail, and the mechanisms of the catalysis of hydrogen production from water have been analyzed based on most recent studies (Eckenhoff et al. 2013; Dempsey et al. 2009; Connolly and Espenson 1986; Artero et al. 2011). In contrast, to the best of our knowledge, there were not many reports in the literature dealing with the dicobaloxime or organodicobaloxime catalysts for chemical fixation of CO₂ to synthesize value-added chemicals. There are several possible approaches for catalytic conversion of CO₂ into desirable products in view of resource utilization and reduce the levels of CO₂ in the atmosphere. One of the most promising strategies in this field has been the synthesis of cyclic carbonates from CO₂ and various epoxides (Anastas and Lankey 2000; Darensbourg and Holtcamp 1996; Cuesta-Aluja et al. 2016; Al-Qaisi et al. 2016; Martinez et al. 2015).

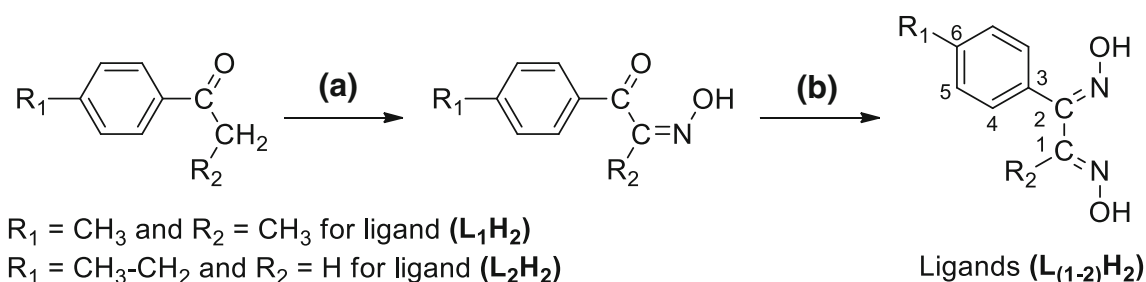
Here, our aim is to draw attention to the organic solvent-free synthesis of cyclic carbonates from chemical fixation

of CO₂ through the assistance of axial ligand-bridged dicobaloxime and organodicobaloximes as homogeneous catalysts. The dicobaloxime or organodicobaloximes are stable-air, low-cost, high activity and easily obtained as compared to the other class metal complexes are surprisingly remained unexplored as catalysts for the transformation of CO₂ to value-added chemicals. These complexes (**1–12**) have been characterized by various spectroscopic methods such as NMR (¹H and ¹³C) spectroscopy, UV–Visible spectroscopy, FT-IR spectroscopy, Mass spectroscopy, molar conductivity analysis, melting point, and magnetic susceptibility experiments with elemental analysis. Also, the redox studies were discussed on a glassy carbon electrode in DMSO in the presence of 0.1 M n-Bu₄NClO₄ as the supporting electrolyte using cyclic voltammetry (CV) methods.

Experimental

General considerations

All chemicals and solvents commercially available were purchased from commercial sources and without the special requirement of any additional chemical process used as received. The NMR (¹H and ¹³C) spectra were recorded in 5 mm tubes at 25 °C with a Bruker Avance 300 NMR at 300 MHz for ¹H and 75 MHz for ¹³C, respectively. The NMR chemical shifts were referenced to the residual solvent as determined relative to TMS ($\delta = 0$ ppm); coupling constants (*J*) are in Hertz with chemical shifts given in ppm at 25 °C. Elemental analyses (C, H, and N) were performed on an LECO CHNS model 932 elemental analyzer. Infrared spectra were obtained on a Perkin-Elmer Two ATR Fourier transform spectrometer in the range of 400–4000 cm⁻¹. UV–Visible spectra were obtained using quartz cells at 25 °C in a Perkin-Elmer model Lambda 25 spectrophotometer in the range of 200–1100 nm and C₂H₅OH with CH₂Cl₂ was used as solvents. Magnetic susceptibilities are measured by the Gouy methods and the experimental results were obtained on a Sherwood Scientific Magnetic Susceptibility Balance (Model MK1) at 25 °C. The compound Hg[Co(SCN)₄] has been preferred as a calibrant and diamagnetic corrections were calculated from Pascal's constants. Melting points of all compounds have been determined in open capillary tubes with an Electrothermal 9100 melting point apparatus and are uncorrected. Molar conductivities (Λ_M) measurements were performed on an Inolab Terminal 740 WTW Series in DMF solvent. The mass spectra (LC–MS) were obtained using an Agilent LC–MS/MS spectrometer. The redox studies were recorded using an EcoChemie Autolab PGSTAT 12 potentiostat/galvanostat (Utrecht, The



Scheme 1 Synthesis of dioxime ligands ($\mathbf{L}_1\mathbf{H}_2$) and ($\mathbf{L}_2\mathbf{H}_2$); **a** $n\text{-C}_4\text{H}_9\text{ONO}$, $\text{C}_2\text{H}_5\text{ONa}$, $-5\text{ }^\circ\text{C}$, **b** CH_3COONa , $\text{NH}_2\text{OH}\cdot\text{HCl}$, EtOH , reflux temperature

Netherlands) with the electrochemical software package 4.9. As the electrode system, 3 mm a GCE working electrode (Bioanalytical Systems, Lafayette, USA), a Pt wire as counter electrode and an Ag/AgCl as reference electrode (Metrohm, Switzerland). Catalytic tests were performed in a PARR 4560 50 mL stainless pressure reactor. Gas chromatography was performed on an Agilent 7820A GC system with nitrogen as the carrier gas. The ligands ($\mathbf{L}_1\mathbf{H}_2$) and ($\mathbf{L}_2\mathbf{H}_2$) were synthesized following the procedure with some modifications (Kilic et al. 2013b, 2014) and briefly the syntheses are given in Scheme 1.

Synthesis of the dicobaloxime complexes (1-6)

The dioxime ligands ($\mathbf{L}_1\mathbf{H}_2$) or ($\mathbf{L}_2\mathbf{H}_2$) (2.30 g, 12.0 mmol) and $\text{CoCl}_2\cdot 6\text{H}_2\text{O}$ (1.43 g, 6.0 mmol) were dissolved in 100 mL of 96% ethanol and stirred for 40 min with occasional swirling under a nitrogen atmosphere. The mixtures turned green immediately. The green reaction mixtures were gradually heated to reflux temperature and maintained at this temperature for 2–3 h. After the green mixtures were allowed to cool to room temperature and 1,6-diaminohexane (**DAH**), 4,4'-bipyridine (**4,4'-bpy**) or 2,4,8,10-tetraoxaspiro[5.5]undecane-3,9-dipropanamine (**TUPA**) (3.0 mmol) was added to mixture as axial-bridged ligand and air was passed through the solution for about 5 h. A desired product was formed as brown precipitate after water (10 mL) addition. Recrystallization from $\text{CH}_2\text{Cl}_2/\text{C}_2\text{H}_5\text{OH}$ by slow evaporation afforded pure compounds obtained. The obtained compounds were washed successively with small amounts of water, and diethyl ether and finally air-dried.

$[(\mathbf{L}_1\mathbf{H})_2\text{CoCl}-(\text{DAH})-\text{CoCl}(\mathbf{L}_1\mathbf{H})_2]$ (1)

Color: brown, yield: 77%, m.p: $185\text{ }^\circ\text{C}$, Anal. Calc. for $[\text{C}_{46}\text{H}_{60}\text{N}_{10}\text{O}_8\text{Cl}_2\text{Co}_2]$ (F.W: 1069.8 g/mol): C, 51.64; H, 5.65; N, 13.09. Found: C, 51.60; H, 5.58; N, 13.04%. $\Lambda_M = 16\ \Omega^{-1}\text{cm}^2\ \text{mol}^{-1}$ (in DMF), $\mu_{\text{eff}} = \text{Dia}$, LC-MS (Scan ES^+): m/z (%) 1069.3 (20) $[\text{M}]^+$. FT-IR (KBr pellet, $\nu_{\text{max}}/\text{cm}^{-1}$): 3582–3108 $\nu(\text{O}-\text{H}\cdots\text{O}/\text{NH}_2)$, 3027 $\nu(\text{Ar}-\text{CH})$,

2952–2856 $\nu(\text{Aliph}-\text{CH})$, 1603 $\nu(\text{C}=\text{N})$, 1557–1446 $\nu(\text{C}=\text{C})$, 1266 $\nu(\text{N}-\text{O})$ and 501 $\nu(\text{Co}-\text{N})$. $^1\text{H-NMR}$ (DMSO-d_6 , TMS, 300 MHz, δ ppm): 18.62 (d, 4H, $J = 8.5\ \text{Hz}$, $\text{O}-\text{H}\cdots\text{O}$), 7.57–6.86 (m, 16H, $\text{Ar}-\text{CH}$), 2.77 (s, 12H, $\text{Ar}-\text{CH}_3$), 2.42 (s, 12H, $\text{C}-\text{CH}_3$) and 2.33–1.24 (m, 16H, NH_2 and $\text{Aliph}-\text{CH}_2$). $^{13}\text{C-NMR}$ (DMSO-d_6 , TMS, 75 MHz, δ ppm): 150.05 ($\underline{\text{C}}_1$ of oxime), 142.83 ($\underline{\text{C}}_2$ of oxime), 139.09 and 138.88 ($\underline{\text{C}}_6$ of Ar), 130.72 and 129.72, ($\underline{\text{C}}_3$ of Ar), 128.96 ($\underline{\text{C}}_4$ of Ar), 128.17 ($\underline{\text{C}}_5$ of Ar), 31.12 ($\text{DAH}-\text{CH}_2$), 21.51 ($\text{Ar}-\text{CH}_3$) and 14.72 ($\text{CH}_3\text{C} = \text{NOH}$). UV-Vis ($\lambda_{\text{max}}/\text{nm}$ ($\log\epsilon$), * = shoulder peak): 253 (4.65), 320 (4.36), 603* and 869* (in $\text{C}_2\text{H}_5\text{OH}$); 254 (4.58), 324 (4.12), 586 (2.58) and 879* (in CH_2Cl_2).

$[(\mathbf{L}_2\mathbf{H})_2\text{CoCl}-(\text{DAH})-\text{CoCl}(\mathbf{L}_2\mathbf{H})_2]$ (2)

Color: brown, yield: 79%, m.p: $189\text{ }^\circ\text{C}$, Anal. Calc. for $[\text{C}_{46}\text{H}_{60}\text{N}_{10}\text{O}_8\text{Cl}_2\text{Co}_2]$ (F.W: 1069.8 g/mol): C, 51.64; H, 5.65; N, 13.09. Found: C, 51.59; H, 5.58; N, 13.13%. $\Lambda_M = 18\ \Omega^{-1}\text{cm}^2\ \text{mol}^{-1}$ (in DMF), $\mu_{\text{eff}} = \text{Dia}$, LC-MS (Scan ES^+): m/z (%) 1069.5 (20) $[\text{M}]^+$. FT-IR (KBr pellet, $\nu_{\text{max}}/\text{cm}^{-1}$): 3543–3104 $\nu(\text{O}-\text{H}\cdots\text{O}/\text{NH}_2)$, 3026 $\nu(\text{Ar}-\text{CH})$, 2963–2870 $\nu(\text{Aliph}-\text{CH})$, 1601 $\nu(\text{C}=\text{N})$, 1551–1456 $\nu(\text{C}=\text{C})$, 1270 $\nu(\text{N}-\text{O})$ and 512 $\nu(\text{Co}-\text{N})$. $^1\text{H-NMR}$ (DMSO-d_6 , TMS, 300 MHz, δ ppm): 20.18 (d, 4H, $J = 7.5\ \text{Hz}$, $\text{O}-\text{H}\cdots\text{O}$), 8.45 (s, 4H, $\text{CH}=\text{N}$), 7.48 (d, 8H, $J = 8.0\ \text{Hz}$, $\text{Ar}-\text{CH}$), 7.23 (d, 8H, $J = 8.0\ \text{Hz}$, $\text{Ar}-\text{CH}$), 2.67–2.56 (q, 8H, CH_3-CH_2) and 1.25–0.84 (m, 28H, CH_3-CH_2 , NH_2 and $\text{Aliph}-\text{CH}_2$). $^{13}\text{C-NMR}$ (DMSO-d_6 , TMS, 75 MHz, δ ppm): 151.24 ($\underline{\text{C}}_1$ of oxime) and 145.01 ($\underline{\text{C}}_2$ of oxime), 141.27 ($\underline{\text{C}}_6$ of Ar), 131.90 ($\underline{\text{C}}_3$ of Ar), 128.21 ($\underline{\text{C}}_4$ of Ar) and 127.72 ($\underline{\text{C}}_5$ of Ar), 31.13 ($\text{DAH}-\text{CH}_2$), 28.39 (CH_3-CH_2) and 15.97 (CH_3-CH_2). UV-Vis [$\lambda_{\text{max}}/\text{nm}$ ($\log\epsilon$): 238 (4.80) and 266 (3.93) (in $\text{C}_2\text{H}_5\text{OH}$); 221 (4.56) and 259 (3.86) (in CH_2Cl_2).

$[(\mathbf{L}_1\mathbf{H})_2\text{CoCl}-(4,4'\text{-bpy})-\text{CoCl}(\mathbf{L}_1\mathbf{H})_2]$ (3)

Color: brown, yield: 78%, m.p: $189\text{ }^\circ\text{C}$, Anal. Calc. for $[\text{C}_{50}\text{H}_{52}\text{N}_{10}\text{O}_8\text{Cl}_2\text{Co}_2]$ (F.W: 1109.8 g/mol): C, 54.11; H, 4.72; N, 12.62. Found: C, 54.07; H, 4.68; N, 12.58%.

$\Lambda_M = 11 \Omega^{-1}\text{cm}^2 \text{mol}^{-1}$ (in DMF), $\mu_{\text{eff}} = \text{Dia}$, LC-MS (Scan ES⁺): *m/z* (%) 1109.7 (20) [M]⁺. FT-IR (KBr pellet, $\nu_{\text{max}}/\text{cm}^{-1}$): 3552-3178 $\nu(\text{O}-\text{H}\cdots\text{O})$, 3082 $\nu(\text{Ar}-\text{CH})$, 2964-2869 $\nu(\text{Aliph}-\text{CH})$, 1604 $\nu(\text{C}=\text{N})$, 1542-1447 $\nu(\text{C}=\text{C})$, 1267 $\nu(\text{N}-\text{O})$ and 515 $\nu(\text{Co}-\text{N})$. ¹H-NMR (DMSO-*d*₆, TMS, 300 MHz, δ ppm): 18.36 (s, 4H, O-*H*⋯O), 8.27 (s, 4H, Ar-*CH*), 7.06 (s, 4H, Ar-*CH*), 7.93 (d, 8H, *J* = 8.5 Hz, Ar-*CH*), 7.73 (d, 8H, *J* = 8.5 Hz, Ar-*CH*), 2.33 (s, 12H, Ar-*CH*₃) and 2.20 (s, 12H, C-*CH*₃). ¹³C-NMR (DMSO-*d*₆, TMS, 75 MHz, δ ppm): 155.47 (*C*₁ of oxime) and 153.83 (*C*₂ of oxime), 152.99 and 152.47 (ortho *C* of 4,4'-bpy), 151.13 (para *C* of 4,4'-bpy), 140.27 (*C*₆ of Ar), 130.74 (*C*₃ of Ar), 129.47 (*C*₄ of Ar), 128.22 (*C*₅ of Ar), 126.72 (meta *C* of 4,4'-bpy), 21.54 (Ar-*CH*₃) and 14.76 (*CH*₃C=NOH). UV-Vis ($\lambda_{\text{max}}/\text{nm}$ (log ϵ), * = shoulder peak): 253 (4.76) and 323 (4.51) (in C₂H₅OH); 234 (4.63), 255 (4.32) and 328* (in CH₂Cl₂).

[(L₂H)₂CoCl-(4,4'-bpy)-CoCl(L₂H)₂] (4)

Color: brown, yield: 80%, m.p: 166 °C, Anal. Calc. for [C₅₀H₅₂N₁₀O₈Cl₂Co₂] (F.W: 1109.8 g/mol): C, 54.11; H, 4.72; N, 12.62. Found: C, 54.04; H, 4.64; N, 12.70%. $\Lambda_M = 16 \Omega^{-1}\text{cm}^2 \text{mol}^{-1}$ (in DMF), $\mu_{\text{eff}} = \text{Dia}$, LC-MS (Scan ES⁺): *m/z* (%) 1109.9 (15) [M]⁺. FT-IR (KBr pellet, $\nu_{\text{max}}/\text{cm}^{-1}$): 3552-3113 $\nu(\text{O}-\text{H}\cdots\text{O})$, 3059 $\nu(\text{Ar}-\text{CH})$, 2964-2872 $\nu(\text{Aliph}-\text{CH})$, 1605 $\nu(\text{C}=\text{N})$, 1534-1456 $\nu(\text{C}=\text{C})$, 1272 $\nu(\text{N}-\text{O})$ and 498 $\nu(\text{Co}-\text{N})$. ¹H-NMR (DMSO-*d*₆, TMS, 300 MHz, δ ppm): 19.02 and 18.83 (s, 4H, O-*H*⋯O), 8.44 (s, 4H, *CH*=N), 8.36-8.13 (m, 8H, Ar-*CH*), 7.47-7.20 (m, 16H, Ar-*CH*), 2.70-2.51 (q, 8H, *CH*₃-*CH*₂) and 1.24-1.15 (m, 12H, *CH*₃-*CH*₂), UV-Vis ($\lambda_{\text{max}}/\text{nm}$ (log ϵ), * = shoulder peak): 237 (4.23), 262 (4.08) and 345* (in C₂H₅OH); 224 (4.33), 255 (4.11), 338* and 409 (3.04) (in CH₂Cl₂).

[(L₁H)₂CoCl-(TUPA)-CoCl(L₁H)₂] (5)

Color: brown, yield: 78%, m.p: 178 °C, Anal. Calc. for [C₅₃H₇₀N₁₀O₁₂Cl₂Co₂] (F.W: 1228.0 g/mol): C, 51.84; H, 5.75; N, 11.41. Found: C, 51.78; H, 5.64; N, 11.37%. $\Lambda_M = 13 \Omega^{-1}\text{cm}^2 \text{mol}^{-1}$ (in DMF), $\mu_{\text{eff}} = \text{Dia}$, LC-MS (Scan ES⁺): *m/z* (%) 1228.1 (20) [M]⁺. FT-IR (KBr pellet, $\nu_{\text{max}}/\text{cm}^{-1}$): 3621-3242 $\nu(\text{O}-\text{H}\cdots\text{O}/\text{NH}_2)$, 3027 $\nu(\text{Ar}-\text{CH})$, 2953-2854 $\nu(\text{Aliph}-\text{CH})$, 1601 $\nu(\text{C}=\text{N})$, 1552-1455 $\nu(\text{C}=\text{C})$, 1268 $\nu(\text{N}-\text{O})$ and 502 $\nu(\text{Co}-\text{N})$. ¹H-NMR (DMSO-*d*₆, TMS, 300 MHz, δ ppm): 18.73 and 18.34 (s, 4H, O-*H*⋯O for *cis* isomer), 18.62 (d, 4H, *J* = 8.8 Hz, O-*H*⋯O for *trans* isomer), 7.59-7.07 (m, 16H, Ar-*CH*), 4.34 (s, 2H, O-*CH*), 4.19 (t, 8H, *J* = 6.0 Hz, O-*CH*₂), 2.78 (s, 12H, Ar-*CH*₃), 2.27 (s, 12H, C-*CH*₃) and 1.74-0.86 (m, 16H, *NH*₂ and Aliph-*CH*₂). ¹³C-NMR (DMSO-*d*₆, TMS, 75 MHz, δ ppm): 153.37 (*C*₁ of oxime), 151.97 (*C*₂ of

oxime), 139.70 and 139.13 (*C*₆ of Ar), 130.73 and 129.62, (*C*₃ of Ar), 129.30 and 128.30 (*C*₄ of Ar), 127.42 (*C*₅ of Ar), 101.38 (O-*CH*), 69.83 (O-*CH*₂), 42.50 (NH₂-*CH*₂), 32.32 (*C*-*CH*₂), 31.40 (CH-*CH*₂), 24.02 (CH₂-*CH*₂-*CH*₂), 21.51 (Ar-*CH*₃) and 14.54 (*CH*₃C=NOH). UV-Vis ($\lambda_{\text{max}}/\text{nm}$ (log ϵ), * = shoulder peak): 251 (4.62), 324 (4.21) and 394* (in C₂H₅OH); 254 (4.43), 330 (4.03) and 407* (in CH₂Cl₂).

[(L₂H)₂CoCl-(TUPA)-CoCl(L₂H)₂] (6)

Color: brown, yield: 80%, m.p: 197 °C, Anal. Calc. for [C₅₃H₇₀N₁₀O₁₂Cl₂Co₂] (F.W: 1228.0 g/mol): C, 51.84; H, 5.75; N, 11.41. Found: C, 51.82; H, 5.77; N, 11.39%. $\Lambda_M = 15 \Omega^{-1}\text{cm}^2 \text{mol}^{-1}$ (in DMF) $\mu_{\text{eff}} = \text{Dia}$, LC-MS (Scan ES⁺): *m/z* (%) 1228.2 (25) [M]⁺. FT-IR (KBr pellet, $\nu_{\text{max}}/\text{cm}^{-1}$): 3553-3121 $\nu(\text{O}-\text{H}\cdots\text{O}/\text{NH}_2)$, 3030 $\nu(\text{Ar}-\text{CH})$, 2963-2871 $\nu(\text{Aliph}-\text{CH})$, 1604 $\nu(\text{C}=\text{N})$, 1513-1456 $\nu(\text{C}=\text{C})$, 1271 $\nu(\text{N}-\text{O})$ and 512 $\nu(\text{Co}-\text{N})$. ¹H-NMR (DMSO-*d*₆, TMS, 300 MHz, δ ppm): 20.02 and 19.98 (s, 4H, O-*H*⋯O), 8.45 (s, 4H, *CH*=N), 7.47 (d, 8H, *J* = 8.1 Hz, Ar-*CH*), 7.22 (d, 8H, *J* = 8.1 Hz, Ar-*CH*), 4.42 (s, 2H, O-*CH*), 4.16 (d, 8H, *J* = 8.6 Hz, O-*CH*₂), 2.76-2.55 (m, 20H, Aliph-*CH*₂) and 1.24-1.06 (m, 16H, *NH*₂ and Aliph-*CH*₃). ¹³C-NMR (DMSO-*d*₆, TMS, 75 MHz, δ ppm): 151.22 (*C*₁ of oxime), 149.99 (*C*₂ of oxime), 141.25 (*C*₆ of Ar), 128.92 and 128.55, (*C*₃ of Ar), 128.32 and 128.18 (*C*₄ of Ar), 127.72 (*C*₅ of Ar), 101.73 (O-*CH*), 69.92 (O-*CH*₂), 56.03 (NH₂-*CH*₂), 31.72 (*C*-*CH*₂), 31.14 (CH-*CH*₂), 28.56 (CH₃-*CH*₂), 22.02 (CH₂-*CH*₂-*CH*₂) and 15.97 (*CH*₃-*CH*₂). UV-Vis ($\lambda_{\text{max}}/\text{nm}$ (log ϵ), * = shoulder peak): 239 (4.60), 264 (4.31) and 381* (3.88) (in C₂H₅OH); 259 (4.42), 341* and 419 (3.74) (in CH₂Cl₂).

Synthesis of the organodicobaloxime complexes (7-12)

To a stirred solution of dicobaloxime (**1-6**) complexes (3.0 mmol) in absolute ethanol (100 mL), NaOH (1.0 g, 25.0 mmol) dissolved in water (10 mL) was then added dropwise at 0 °C with stirring for 20 min. under a N₂ atmosphere. Then, sodium borohydride (NaBH₄) (1.90 g, 4.0 mmol) dissolved in water (10 mL) was added to the mixture by dropping cone. During this period, the reaction mixture turned from brown to dark blue, followed by its immediately turning orange on the addition of benzyl bromide (4.26 g, 24.8 mmol). The reaction mixture was stirred at 0 °C for 4 h, and then the solutions were removed under N₂ atmosphere. The reaction mixture was opened to air and acetone (10 mL) with water (10 mL) was added dropwise. The volume of the reaction mixture was reduced 10 mL by evaporation and then poured into 40 mL of

water. The solution was concentrated, filtered and washed with hexane and diethyl ether, and dried. The obtained pure compounds were recrystallized from $\text{CHCl}_3/\text{C}_2\text{H}_5\text{OH}$ (1:2) solution and finally dried *in vacuo*.

$[(L_1H)_2PhCH_2Co-(DAH)-CoCH_2Ph(L_1H)_2]$ (7)

Color: gold yellow, yield (%): 68, m.p: 140 °C, Anal. Calc. for $[\text{C}_{60}\text{H}_{74}\text{N}_{10}\text{O}_8\text{Co}_2]$ (F.W: 1181.2 g/mol): C, 61.01; H, 6.32; N, 11.86 Found: C, 60.93; H, 6.26; N, 11.79%. $\Lambda_M = 17 \Omega^{-1}\text{cm}^2 \text{mol}^{-1}$ (in DMF), $\mu_{\text{eff}} = \text{Dia}$, LC-MS (Scan ES^+): m/z (%) 1181.5 (20) $[\text{M}^+]$. FT-IR (KBr pellet, $\nu_{\text{max}}/\text{cm}^{-1}$): 3552-3160 $\nu(\text{O}-\text{H}\cdots\text{O}/\text{NH}_2)$, 3060 and 3030 $\nu(\text{Ar}-\text{CH})$, 2960-2865 $\nu(\text{Aliph}-\text{CH})$, 1601 $\nu(\text{C}=\text{N})$, 1537-1455 $\nu(\text{C}=\text{C})$, 1262 $\nu(\text{N}-\text{O})$ and 498 $\nu(\text{Co}-\text{N})$. $^1\text{H-NMR}$ (DMSO- d_6 , TMS, 300 MHz, δ ppm): 7.72-6.96 (m, 26H, Ar- $\underline{\text{CH}}$), 5.16 (s, 4H, Ph- $\underline{\text{CH}_2}$), 2.37 (s, 12H, Ar- $\underline{\text{CH}_3}$), 2.14 (s, 12H, C- $\underline{\text{CH}_3}$) and 1.73-0.87 (m, 16H, $\underline{\text{NH}_2}$ and Aliph- $\underline{\text{CH}_2}$). UV-Vis ($\lambda_{\text{max}}/\text{nm}$ (log ϵ), * = shoulder peak): 250 (4.83), 320 (4.26) and 428* (in $\text{C}_2\text{H}_5\text{OH}$); 251 (4.76), 324 (4.23) and 435* (in CH_2Cl_2).

$[(L_2H)_2PhCH_2Co-(DAH)-CoCH_2Ph(L_2H)_2]$ (8)

Color: gold yellow, yield (%): 72, m.p: 149 °C, Anal. Calc. for $[\text{C}_{60}\text{H}_{74}\text{N}_{10}\text{O}_8\text{Co}_2]$ (F.W: 1181.2 g/mol): C, 61.01; H, 6.32; N, 11.86 Found: C, 60.92; H, 6.20; N, 11.78%. $\Lambda_M = 13 \Omega^{-1}\text{cm}^2 \text{mol}^{-1}$ (in DMF), $\mu_{\text{eff}} = \text{Dia}$, LC-MS (Scan ES^+): m/z (%) 1182.2 (17) $[\text{M} + \text{H}^+]$. FT-IR (KBr pellet, $\nu_{\text{max}}/\text{cm}^{-1}$): 3539-3152 $\nu(\text{O}-\text{H}\cdots\text{O}/\text{NH}_2)$, 3056 and 3029 $\nu(\text{Ar}-\text{CH})$, 2962-2871 $\nu(\text{Aliph}-\text{CH})$, 1602 $\nu(\text{C}=\text{N})$, 1559-1454 $\nu(\text{C}=\text{C})$, 1269 $\nu(\text{N}-\text{O})$ and 508 $\nu(\text{Co}-\text{N})$. $^1\text{H-NMR}$ (DMSO- d_6 , TMS, 300 MHz, δ ppm): 8.55 (s, 4H, $\underline{\text{CH}}=\text{N}$), 7.47-7.26 (m, 26H, Ar- $\underline{\text{CH}}$), 5.18 (s, 4H, Ph- $\underline{\text{CH}_2}$), 2.65-2.61 (q, 8H, $\underline{\text{CH}_3}-\underline{\text{CH}_2}$) and 1.39-0.86 (m, 28H, $\underline{\text{CH}_3}-\underline{\text{CH}_2}$, $\underline{\text{NH}_2}$ and Aliph- $\underline{\text{CH}_2}$). $^{13}\text{C-NMR}$ (DMSO- d_6 , TMS, 75 MHz, δ ppm): 150.00 ($\underline{\text{C}}_1$ of oxime) and 145.23 ($\underline{\text{C}}_2$ of oxime), 141.92 ($\underline{\text{C}}_6$ of Ar), 140.91 ($\underline{\text{C}}_1$ of phenyl), 137.63 (ortho $\underline{\text{C}}$ of phenyl), 136.08 ($\underline{\text{C}}_3$ of Ar), 130.89 (para $\underline{\text{C}}$ of phenyl), 128.83 ($\underline{\text{C}}_4$ of Ar), 128.87 ($\underline{\text{C}}_5$ of Ar), 127.44 (meta $\underline{\text{C}}$ of phenyl), 77.34 (Ph- $\underline{\text{CH}_2}$), 31.70 (DAH- $\underline{\text{CH}_2}$), 28.37 ($\underline{\text{CH}_3}-\underline{\text{CH}_2}$) and 15.91 ($\underline{\text{CH}_3}-\underline{\text{CH}_2}$). UV-Vis ($\lambda_{\text{max}}/\text{nm}$ (log ϵ), * = shoulder peak): 264 (4.48) and 382* (in $\text{C}_2\text{H}_5\text{OH}$); 266 (4.58) and 385* (in CH_2Cl_2).

$[(L_1H)_2PhCH_2Co-(4,4'-bpy)-CoCH_2Ph(L_1H)_2]$ (9)

Color: gold yellow, yield (%): 69, m.p: 129 °C, Anal. Calc. for $[\text{C}_{64}\text{H}_{66}\text{N}_{10}\text{O}_8\text{Co}_2]$ (F.W: 1221.1 g/mol): C, 62.95; H, 5.45; N, 11.47 Found: C, 62.88; H, 5.38; N, 11.40%. $\Lambda_M = 14 \Omega^{-1}\text{cm}^2 \text{mol}^{-1}$ (in DMF), $\mu_{\text{eff}} = \text{Dia}$, LC-MS (Scan ES^+): m/z (%) 1221.3 (15) $[\text{M}^+]$. FT-IR (KBr pellet, $\nu_{\text{max}}/\text{cm}^{-1}$): 3576-3160 $\nu(\text{O}-\text{H}\cdots\text{O})$, 3056 and 3031 $\nu(\text{Ar}-$

CH), 2956-2865 $\nu(\text{Aliph}-\text{CH})$, 1603 $\nu(\text{C}=\text{N})$, 1536-1456 $\nu(\text{C}=\text{C})$, 1264 $\nu(\text{N}-\text{O})$ and 502 $\nu(\text{Co}-\text{N})$. $^1\text{H-NMR}$ (DMSO- d_6 , TMS, 300 MHz, δ ppm): 18.80 and 18.48 (s, 4H, O- $\underline{\text{H}}\cdots\text{O}$), 8.56 (s, 4H, Ar- $\underline{\text{CH}}$), 8.05 (s, 4H, Ar- $\underline{\text{CH}}$), 7.93 (d, 8H, $J = 7.5$ Hz, Ar- $\underline{\text{CH}}$), 7.72 (d, 8H, $J = 7.5$ Hz, Ar- $\underline{\text{CH}}$), 7.32-7.06 (m, 10H, Ar- $\underline{\text{CH}}$), 5.13 (s, 4H, Ph- $\underline{\text{CH}_2}$), 2.42 (s, 12H, Ar- $\underline{\text{CH}_3}$) and 2.32 (s, 12H, C- $\underline{\text{CH}_3}$). $^{13}\text{C-NMR}$ (DMSO- d_6 , TMS, 75 MHz, δ ppm): 158.41 ($\underline{\text{C}}_1$ of oxime) and 155.88 ($\underline{\text{C}}_2$ of oxime), 154.09 (ortho $\underline{\text{C}}$ of 4,4'-bpy), 153.37 (para $\underline{\text{C}}$ of 4,4'-bpy), 150.48 ($\underline{\text{C}}_6$ of Ar), 140.11 ($\underline{\text{C}}_1$ of phenyl), 132.18 (ortho $\underline{\text{C}}$ of phenyl), 130.74 ($\underline{\text{C}}_3$ of Ar), 130.63 (para $\underline{\text{C}}$ of phenyl), 129.96 and 129.64 ($\underline{\text{C}}_4$ of Ar), 129.11 and 128.59 ($\underline{\text{C}}_5$ of Ar), 126.88 (meta $\underline{\text{C}}$ of 4,4'-bpy), 126.08 (meta $\underline{\text{C}}$ of phenyl), 78.16 (Ph- $\underline{\text{CH}_2}$), 21.46 (Ar- $\underline{\text{CH}_3}$) and 15.64 ($\underline{\text{CH}_3}\text{C}=\text{NOH}$). UV-Vis ($\lambda_{\text{max}}/\text{nm}$ (log ϵ), * = shoulder peak): 254 (3.94) and 358* (in $\text{C}_2\text{H}_5\text{OH}$); 234 (4.53), 255 (3.92) and 358* (in CH_2Cl_2).

$[(L_2H)_2PhCH_2Co-(4,4'-bpy)-CoCH_2Ph(L_2H)_2]$ (10)

Color: gold yellow, yield (%): 68, m.p: > 300 °C, Anal. Calc. for $[\text{C}_{64}\text{H}_{66}\text{N}_{10}\text{O}_8\text{Co}_2]$ (F.W: 1221.1 g/mol): C, 62.95; H, 5.45; N, 11.47 Found: C, 62.86; H, 5.34; N, 11.42%. $\Lambda_M = 11 \Omega^{-1}\text{cm}^2 \text{mol}^{-1}$ (in DMF), $\mu_{\text{eff}} = \text{Dia}$, LC-MS (Scan ES^+): m/z (%) 1221.1 (25) $[\text{M}^+]$. FT-IR (KBr pellet, $\nu_{\text{max}}/\text{cm}^{-1}$): 3539-3160 $\nu(\text{O}-\text{H}\cdots\text{O})$, 3029 $\nu(\text{Ar}-\text{CH})$, 2963-2871 $\nu(\text{Aliph}-\text{CH})$, 1598 $\nu(\text{C}=\text{N})$, 1534-1457 $\nu(\text{C}=\text{C})$, 1270 $\nu(\text{N}-\text{O})$ and 508 $\nu(\text{Co}-\text{N})$. $^1\text{H-NMR}$ (DMSO- d_6 , TMS, 300 MHz, δ ppm): 18.42 and 18.13 (s, 4H, O- $\underline{\text{H}}\cdots\text{O}$), 10.03 (s, 4H, $\underline{\text{CH}}=\text{N}$), 8.34 (s, 4H, Ar- $\underline{\text{CH}}$), 7.93 (d, 8H, $J = 7.2$ Hz, Ar- $\underline{\text{CH}}$), 7.72 (d, 8H, $J = 7.2$ Hz, Ar- $\underline{\text{CH}}$), 7.62 (t, 8H, $J = 7.1$ Hz, Ar- $\underline{\text{CH}}$), 7.25 (s, 4H, Ar- $\underline{\text{CH}}$), 7.17 (s, 2H, Ar- $\underline{\text{CH}}$), 5.51 (s, 4H, Ph- $\underline{\text{CH}_2}$), 1.25-1.08 (m, 8H, $\underline{\text{CH}_3}-\underline{\text{CH}_2}$) and 0.87 (s, 12H, $\underline{\text{CH}_3}-\underline{\text{CH}_2}$). UV-Vis ($\lambda_{\text{max}}/\text{nm}$ (log ϵ), * = shoulder peak): 243 (4.86), 272 (3.87) and 381* (in $\text{C}_2\text{H}_5\text{OH}$); 248 (4.49), 269 (3.96) and 384* (in CH_2Cl_2).

$[(L_1H)_2PhCH_2Co-(TUPA)-CoCH_2Ph(L_1H)_2]$ (11)

Color: gold yellow, yield (%): 70, m.p: > 300 °C, Anal. Calc. for $[\text{C}_{67}\text{H}_{84}\text{N}_{10}\text{O}_{12}\text{Co}_2]$ (F.W: 1339.3 g/mol): C, 60.08; H, 6.32; N, 10.46 Found: C, 60.02; H, 6.25; N, 10.38%. $\Lambda_M = 14 \Omega^{-1}\text{cm}^2 \text{mol}^{-1}$ (in DMF), $\mu_{\text{eff}} = \text{Dia}$, LC-MS (Scan ES^+): m/z (%) 1339.4 (25) $[\text{M}^+]$. FT-IR (KBr pellet, $\nu_{\text{max}}/\text{cm}^{-1}$): 3517-3126 $\nu(\text{O}-\text{H}\cdots\text{O}/\text{NH}_2)$, 3060 and 3030 $\nu(\text{Ar}-\text{CH})$, 2952-2859 $\nu(\text{Aliph}-\text{CH})$, 1601 $\nu(\text{C}=\text{N})$, 1557-1454 $\nu(\text{C}=\text{C})$, 1262 $\nu(\text{N}-\text{O})$ and 500 $\nu(\text{Co}-\text{N})$. $^1\text{H-NMR}$ (DMSO- d_6 , TMS, 300 MHz, δ ppm): 7.70-6.73 (m, 26H, Ar- $\underline{\text{CH}}$), 5.15 (s, 4H, Ph- $\underline{\text{CH}_2}$), 4.31 (s, 2H, O- $\underline{\text{CH}}$), 4.22 (t, 8H, $J = 6.2$ Hz, O- $\underline{\text{CH}_2}$), 2.67 (s, 12H, Ar- $\underline{\text{CH}_3}$), 2.33 (s, 12H, C- $\underline{\text{CH}_3}$) and 2.12-0.87 (m, 16H, $\underline{\text{NH}_2}$ and Aliph- $\underline{\text{CH}_2}$). $^{13}\text{C-NMR}$ (DMSO- d_6 , TMS,

75 MHz, δ ppm): 155.23 (C_1 of oxime), 154.51 (C_2 of oxime), 153.08 (ortho C of phenyl), 151.14 (para C of phenyl), 141.32 (C_1 of phenyl), 138.93 (C_6 of Ar), 131.86 and 130.53, (C_3 of Ar), 129.78 (C_4 of Ar), 128.46 (C_5 of Ar), 126.32 (meta C of phenyl), 101.12 (O- \underline{CH}), 77.26 (Ph- $\underline{CH_2}$), 68.58 (O- $\underline{CH_2}$), 42.58 (NH $_2$ - $\underline{CH_2}$), 32.13 ($\underline{C-CH_2}$), 29.75 (CH- $\underline{CH_2}$), 24.21 (CH $_2$ - $\underline{CH_2-CH_2}$), 21.54 (Ar- $\underline{CH_3}$) and 14.48 ($\underline{CH_3C=NOH}$). UV-Vis (λ_{\max}/nm (log ϵ), * = shoulder peak): 251 (4.72), 323 (4.53) and 432* (in C $_2$ H $_5$ OH), 252 (4.41), 315 (4.13) and 438* (in CH $_2$ Cl $_2$).

[(L $_2$ H) $_2$ PhCH $_2$ Co-(TUPA)-CoCH $_2$ Ph(L $_2$ H) $_2$] (12)

Color: gold yellow, yield (%): 64, m.p: 189 °C, Anal. Calc. for [C $_{67}$ H $_{84}$ N $_{10}$ O $_{12}$ Co $_2$] (F.W: 1339.3 g/mol): C, 60.08; H, 6.32; N, 10.46 Found: C, 60.03; H, 6.24; N, 10.52%. $\Lambda_M = 12 \Omega^{-1}\text{cm}^2 \text{mol}^{-1}$ (in DMF), $\mu_{\text{eff}} = \text{Dia}$, LC-MS (Scan ES $^+$): m/z (%) 1339.2 (25) [M $^+$]. FT-IR (KBr pellet, $\nu_{\max}/\text{cm}^{-1}$): 3534-3151 $\nu(\text{O-H}\cdots\text{O}/\text{NH}_2)$, 3029 $\nu(\text{Ar-CH})$, 2964-2871 $\nu(\text{Aliph-CH})$, 1607 $\nu(\text{C=N})$, 1511-1455 $\nu(\text{C=C})$, 1270 $\nu(\text{N-O})$ and 511 $\nu(\text{Co-N})$. $^1\text{H-NMR}$ (DMSO- d_6 , TMS, 300 MHz, δ ppm): 8.52 (s, 4H, $\underline{CH} = \text{N}$), 7.36-7.18 (m, 26H, Ar- \underline{CH}), 5.24 (s, 4H, Ph- $\underline{CH_2}$), 4.28 (s, 2H, O- \underline{CH}), 4.17 (d, 8H, $J = 11.7$ Hz, O- $\underline{CH_2}$), 2.62-2.33 (m, 20H, Aliph- $\underline{CH_2}$) and 1.48-0.86 (m, 16H, NH $_2$ and Aliph- $\underline{CH_3}$). $^{13}\text{C-NMR}$ (DMSO- d_6 , TMS, 75 MHz, δ ppm): 148.44 (C_1 of oxime), 145.76 (C_2 of oxime), 141.93 (ortho C of phenyl), 140.98 (para C of phenyl), 141.32 (C_1 of phenyl), 130.42 (C_6 of Ar), 129.91 and 129.48 (C_3 of Ar), 128.96 and 128.87 (C_4 of Ar), 127.14 (C_5 of Ar), 102.39 (O- \underline{CH}), 77.41 (Ph- $\underline{CH_2}$), 70.07 (O- $\underline{CH_2}$), 58.16 (NH $_2$ - $\underline{CH_2}$), 31.95 ($\underline{C-CH_2}$), 30.94 (CH- $\underline{CH_2}$), 28.76 (CH $_3$ - $\underline{CH_2}$), 21.01 (CH $_2$ - $\underline{CH_2-CH_2}$) and 15.41 ($\underline{CH_3-CH_2}$). UV-Vis (λ_{\max}/nm (log ϵ), * = shoulder peak): 265 (4.48) and 381* (in C $_2$ H $_5$ OH); 268 (4.32) and 389* (in CH $_2$ Cl $_2$).

General procedure of coupling reaction of epoxides and CO $_2$

In a 50-mL stainless-steel autoclave with a magnetic stirring bar in the absence of a solvent and a presence Lewis base (9.0×10^{-5} mol) under CO $_2$ pressure, with a 4.5×10^{-5} mol dicobaloxime or organodicobaloxime complexes and 4.5×10^{-2} mol epoxide was added. The mixture was injected into the reactor which was dried before use. The reaction was carried out under a constant pressure of carbon dioxide and the reaction mixture was stirred at 100 °C for the desired time under an atmosphere of CO $_2$ (99.999%). After the reaction, the mixture was cooled to room temperature and ethylene glycol dibutyl ether added as internal standard for GC (Agilent 7820A) analysis yield determination. All the yields were based on

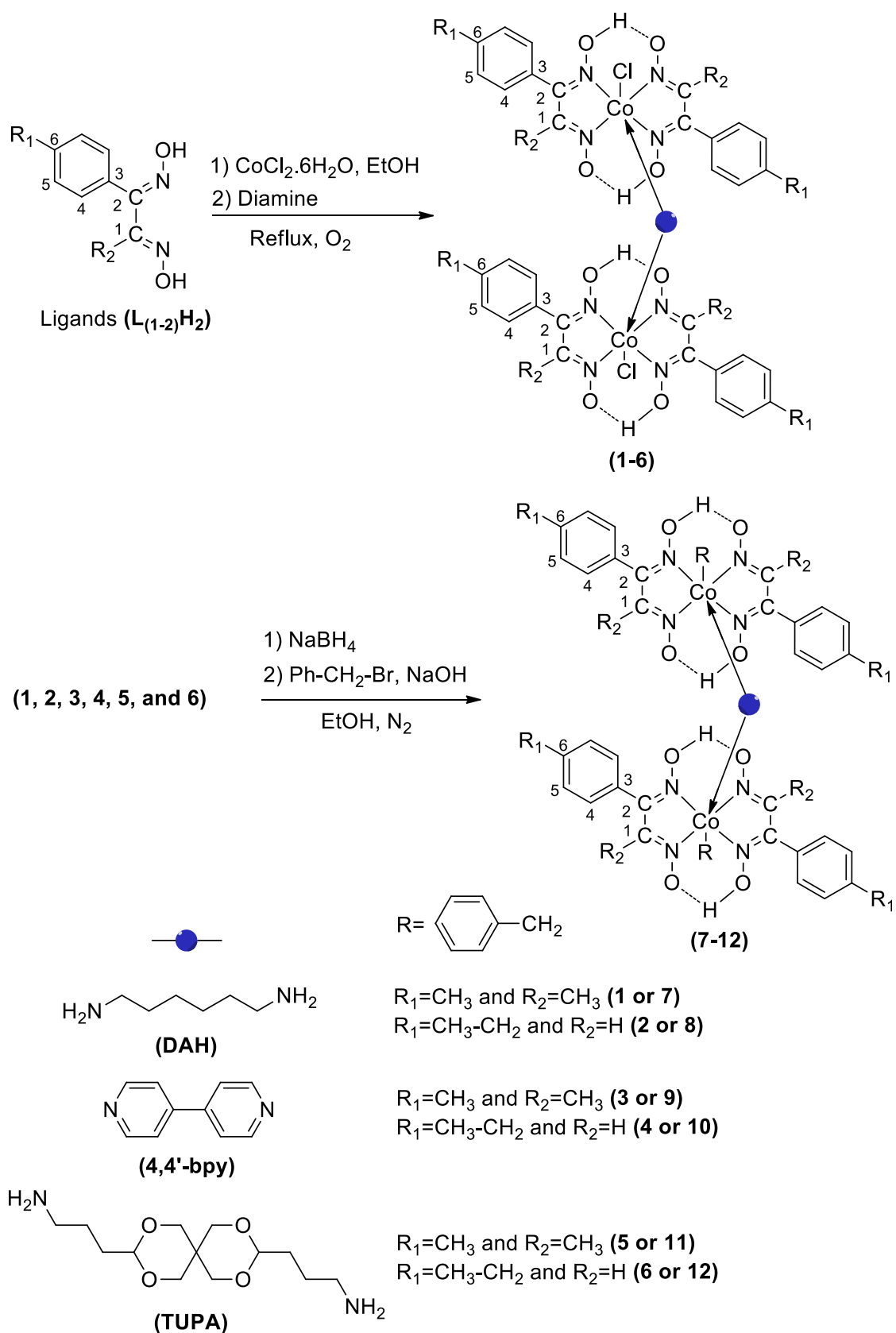
epoxide. The obtained cyclic carbonate in DMSO- d_6 was analyzed by $^1\text{H-NMR}$ and FT-IR spectra. These spectral results show that any polycarbonate, epoxides, DMAP (4-dimethylamino pyridine) or other by-products were not formed significant amounts. Besides, a detailed FT-IR survey shows that the peak at around 1795 cm^{-1} was attributed to the carbonyl group in cyclic carbonate. Also, no peak at 1749 cm^{-1} was detected, which was attributed to the carbonyl group in polycarbonate (Wang et al. 2015).

Results and discussion

Herein, first we reported the synthesis of the two dioxime ligands (**L $_1$ H $_2$** and **L $_2$ H $_2$**) from various ketones skeletons are outlined in Scheme 1. As shown in Scheme 2, the dicobaloxime/organodicobaloxime (**1-12**) complexes were obtained at reflux temperature and under the basic conditions. Dicobaloxime complexes (**1-6**) have been synthesized by treating dioxime ligands (**L $_1$ H $_2$** and **L $_2$ H $_2$**) with CoCl $_2$.6H $_2$ O in the presence of O $_2$ and various diamines under an inert atmosphere. In contrast, organodicobaloxime complexes (**7-12**) synthesized by treating dicobaloxime complexes (**1-6**) with benzyl bromide in the presence of NaBH $_4$ and NaOH in EtOH solvent under an inert atmosphere. These Co(III) complexes (**1-12**) were successfully synthesized and characterized by various spectroscopic methods such as NMR (^1H and ^{13}C) spectroscopy, UV-Visible spectroscopy, FT-IR spectroscopy, Mass spectroscopy, molar conductivity analysis, melting point, and magnetic susceptibility experiments with elemental analysis and cyclic voltammetry (CV). We have attempted to prepare single crystals of dicobaloxime/organodicobaloximes (**1-12**) complexes in various solvents, but unfortunately we could not obtain single crystals suitable for X-ray diffraction studies for all dicobaloxime/organodicobaloximes (**1-12**) complexes.

Spectroscopic properties

The FT-IR spectra of the dicobaloxime/organodicobaloximes (**1-12**) complexes are compared with those of the free dioxime ligands (**L $_1$ H $_2$**) and (**L $_2$ H $_2$**) and their relative frequency and also the assignments are consistent with reported compounds (Figs. 1, 2). In the FT-IR of the dicobaloxime/organodicobaloxime (**1-12**) complexes, the main stretching vibration for intermolecular H-bond (O-H \cdots O), which on an encapsulation of the NH $_2$ groups are observed at 3621-3104 cm^{-1} , provided the first evidence of successful complexation on the Co(III) center in N $_4$ -oxime core. The other important peak due to azomethine $\nu(\text{C=N})$ groups were observed at 1611-1609 cm^{-1} in the FT-IR spectra of the dioxime ligands (**L $_1$ H $_2$**) and (**L $_2$ H $_2$**),



Scheme 2 The structure of the proposed dicobaloxime/organodicobaloximes (**1–12**) complexes

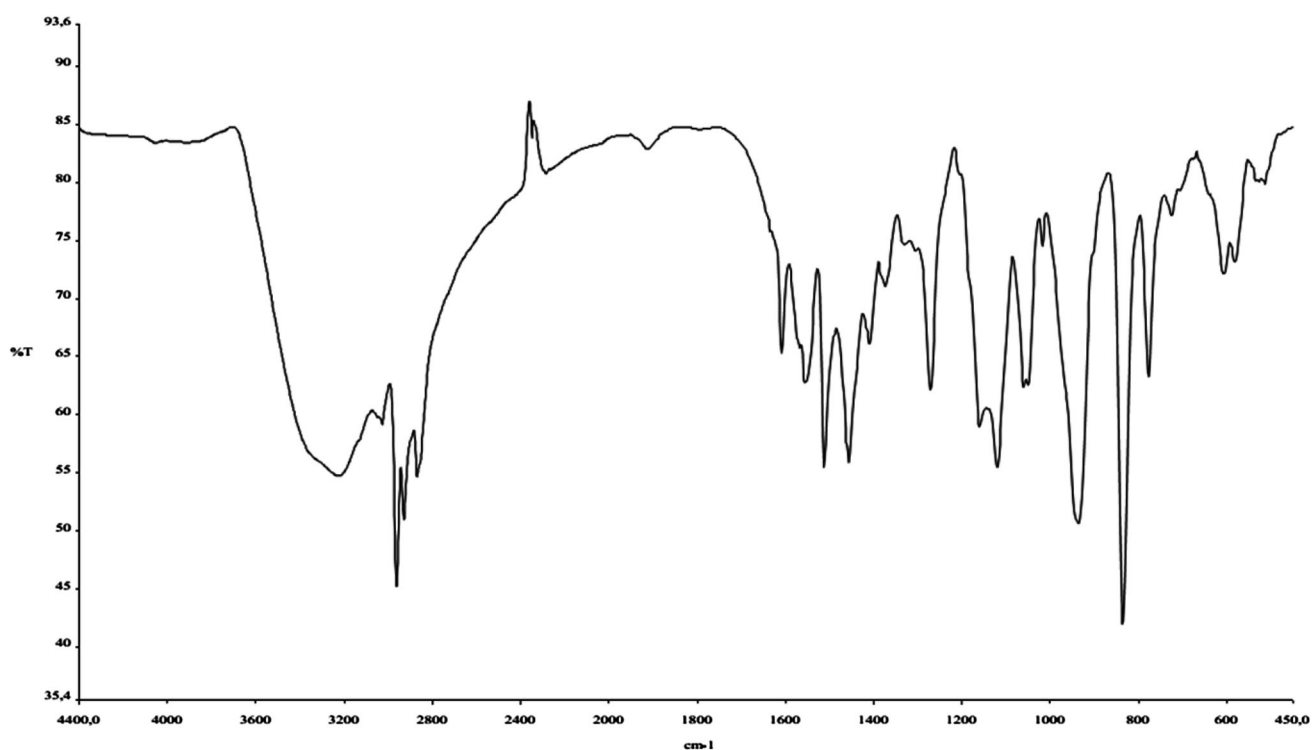


Fig. 1 The FT-IR spectra of dicobaloxime (6) complex

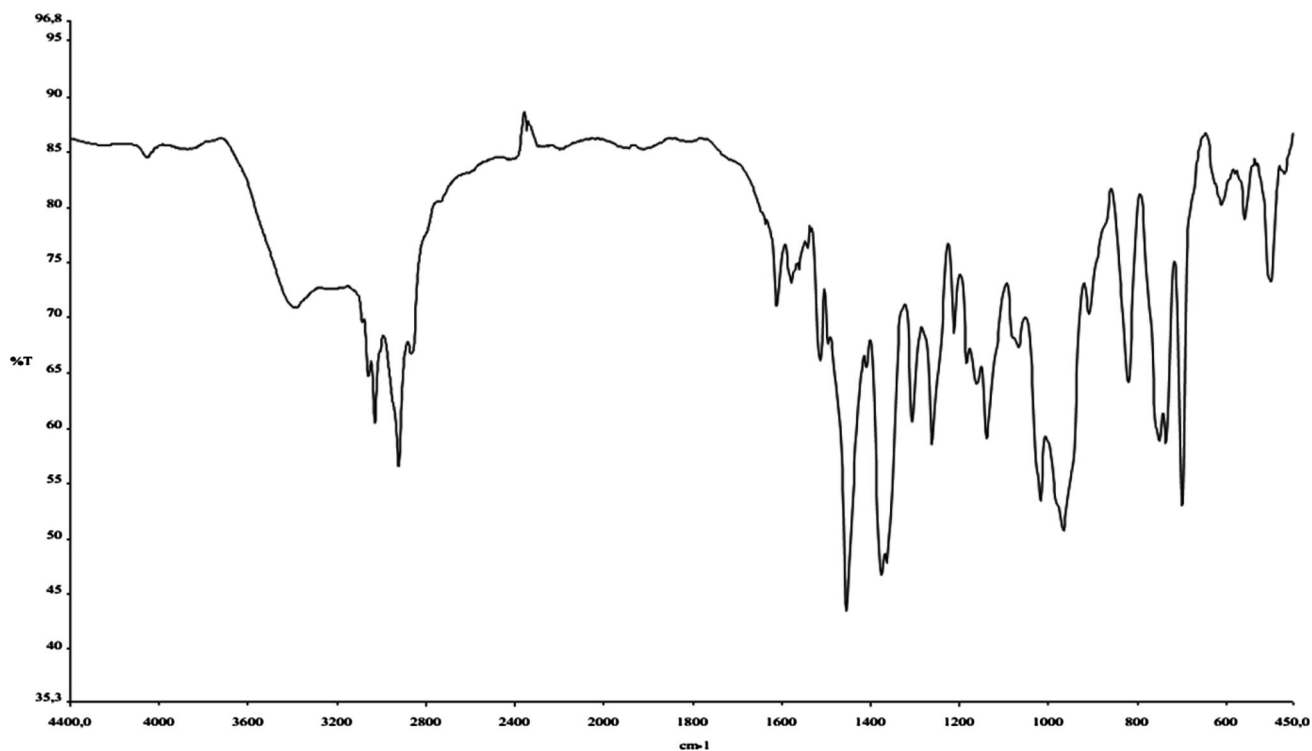


Fig. 2 The FT-IR spectra of organodicobaloxime (7) complex

whereas in the FT-IR of dicobaloxime/organodicobaloximes (1–12), this band observed at $1605\text{--}1598\text{ cm}^{-1}$ a small frequency shift in its position

according to the stretching vibration of ligands (Wani et al. 2016). This a small frequency shift in its position may be because of the formation of $\text{Co(III)} \leftarrow \text{N}$ dative bond in

these complexes as expected. The infrared spectra show that the typical characteristic $\nu(\text{N}-\text{O})$ stretches at about $\sim 1285 \text{ cm}^{-1}$ in ligands (L_1H_2) and (L_2H_2) a small low-frequency shift upon treatment with Co^{3+} ions, supporting the formation of dicobaloxime/organodicobaloximes (**1–12**) complexes. The coordination mode of the ligands (L_1H_2) and (L_2H_2) are further supported by new frequencies occurring in the range $515\text{--}498 \text{ cm}^{-1}$ due to $\nu(\text{Co} \leftarrow \text{N})$ stretching vibrations that are not observed in the FT-IR of the ligands (L_1H_2) and (L_2H_2).

The electronic absorption spectra of the ligands (L_1H_2) and (L_2H_2) and their dicobaloxime/organodicobaloxime (**1–12**) complexes obey well Lambert–Beer's law in the concentration range studied ($2.10^{-6}\text{--}2.10^{-8} \text{ mol L}^{-1}$) in $\text{C}_2\text{H}_5\text{OH}$ and CH_2Cl_2 solution and recorded in the range $200\text{--}1100 \text{ nm}$ at room temperature, suggesting that no other chemical event occurs within this concentration range in $\text{C}_2\text{H}_5\text{OH}$ and CH_2Cl_2 . The UV–Vis absorption bands of the examples (L_1H_2) and (L_2H_2) and their dicobaloxime/organodicobaloximes (**1–12**) indicate similar features for $\pi \rightarrow \pi^*$ or $n \rightarrow \pi^*$ transitions of the chromophoric groups present in the structure of the ligands. The ligands (L_1H_2) and (L_2H_2) and their complexes (**1–12**) show sharp and strong absorption bands under 382 nm in $\text{C}_2\text{H}_5\text{OH}$ and under 385 nm in CH_2Cl_2 are assumed to be probably intra ligand property and can be assigned to the $\pi \rightarrow \pi^*$ or $n \rightarrow \pi^*$ transitions localized on the conjugated aromatic rings and functional azomethine ($\text{C}=\text{N}$) groups, considering their intense and structured absorption band. Another decisive evident bands for the formation of these complexes (**1–12**) observed at $438\text{--}394 \text{ nm}$ can be presumably ascribed to the intermolecular transition from the ligand compounds to the vacant orbitals localized on the coordinated cobaloxime center. One of the most important absorption bands for such molecules is d–d transition in the visible region. But we did not observe these transitions in the all dicobaloxime and organocobaloximes probably due to their very low molar absorption coefficient. However, the dicobaloxime complex (**1**) at high concentrations of showed d–d transitions in the region $586\text{--}879 \text{ nm}$ due to Co^{3+} metal center of cobaloximes (Lever 1968; Moore and Janes 2004).

The ^1H and ^{13}C -NMR chemical results for the ligands (L_1H_2) and (L_2H_2) and their dicobaloxime/organodicobaloxime (**1–12**) complexes are given in the experimental section and Figs. 3, 4, 5 and 6. The ^1H and ^{13}C -NMR values are in good agreement with those obtained for the ligands (L_1H_2) and (L_2H_2) and their cobaloxime complexes (**1–12**). In the ^1H NMR spectra of dioxime ligand (L_1H_2) and (L_2H_2), the D_2O -exchangeable protons of the ($\text{C}=\text{N}-\text{OH}$) groups show chemical shifts at 11.45 ppm as singlet for ligand (L_1H_2) and at 11.86 ppm (*trans* isomer) and 11.69 with 11.47 ppm (*cis* isomer) as

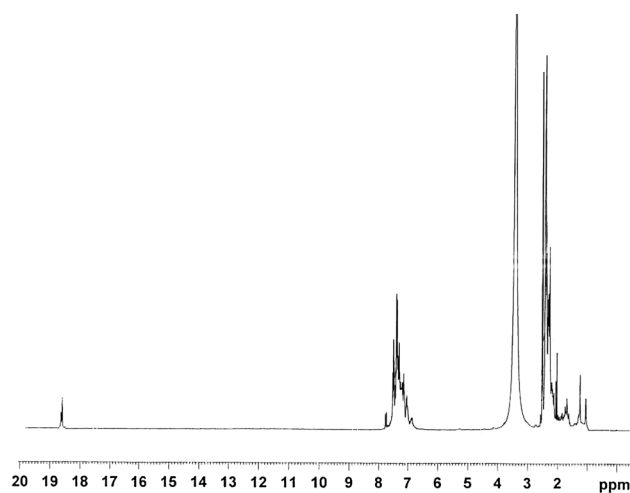


Fig. 3 The ^1H -NMR spectra of dicobaloxime (**1**) complex in DMSO

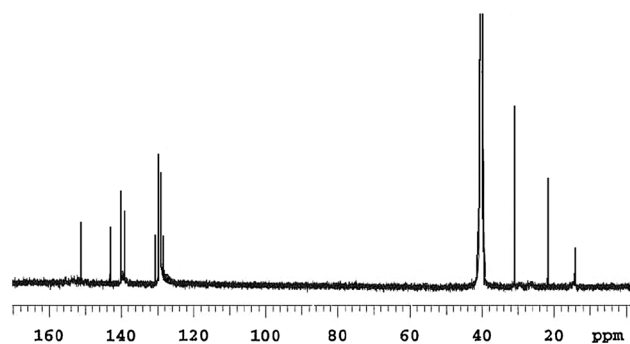


Fig. 4 The ^{13}C -NMR spectra of dicobaloxime (**1**) complex in DMSO

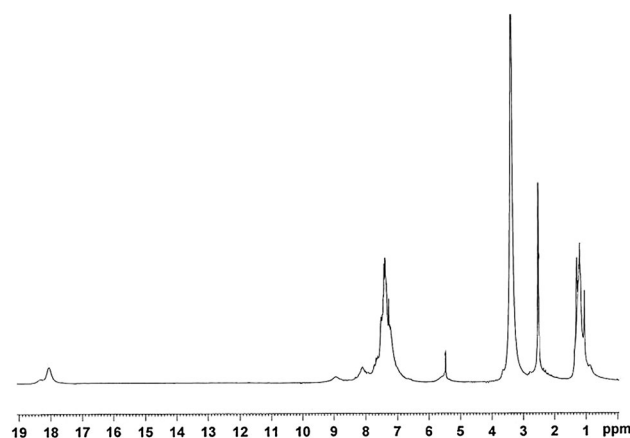


Fig. 5 The ^1H -NMR spectra of organodicobaloxime (**9**) complex in DMSO

singlet for ligand (L_2H_2), consecutively. This peak disappeared in the ^1H -NMR spectrum of dicobaloxime/organodicobaloxime (**1–12**) complexes, while new peaks were observed and identified as two singlet or doublet peaks at range $20.18\text{--}18.33 \text{ ppm}$ for *cis/trans* isomer, indicating that the ($\text{C}=\text{N}-\text{OH}$) groups of dioxime ligands

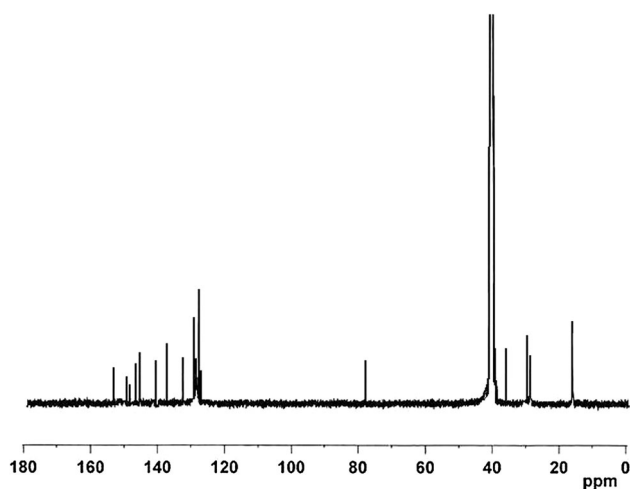


Fig. 6 The ^{13}C -NMR spectra of organodicobaloxime (**9**) complex in DMSO

have been transformed to intramolecular D_2O -exchangeable H-bridge ($\text{O}-\underline{\text{H}}\cdots\text{O}$), supporting the formation of the dicobaloxime/organodicobaloximes (**1–12**) (Mirra et al. 2016). The NMR spectra of dicobaloxime (**1–6**) complexes compared with organodicobaloxime (**7–12**) complexes were found major differences was the presence of a benzyl group connecting instead of a chlorine atom as axial ligand in the organodicobaloxime (**7–12**) complexes. The conversions of the dicobaloxime (**1–6**) complexes to the organodicobaloxime (**7–12**) complexes were confirmed by the changes observed in the NMR spectra and by the appearance of a characteristic singlet resonance at range 5.24–5.13 ppm in the ^1H NMR spectra and also at range 78.16–77.26 ppm in the ^{13}C NMR spectra attributed to the $\text{Ph}-\underline{\text{C}}\text{H}_2$ of the benzyl group as axial ligand. Another decisive event, the signals of the azomethine carbon ($\underline{\text{C}}=\text{N}$) are observed at between 158.41 and 142.83 ppm for the complexes (**1–12**), while this carbon peak is observed at 155.59–145.02 ppm for the dioxime ligand (**L₁H₂**) and (**L₂H₂**) (Yamuna et al., 2016). For corroborate the proposed dimeric cobaloxime structures, The ^1H NMR resonance of axial-bridged ligands (1,6-diaminohexane (**DAH**), 4,4'-bipyridine (**4,4'-bpy**) and 2,4,8,10-tetraoxaspiro[5.5]undecane-3,9-dipropanamine (**TUPA**) were located at range 2.33–1.24 ppm assigned to the $\underline{\text{N}}\text{H}_2$ and $\text{Aliph}-\underline{\text{C}}\text{H}_2$ of axial **DAH** ligand, at range 2.33–0.84 ppm assigned to the $\underline{\text{N}}\text{H}_2$ and $\text{Aliph}-\underline{\text{C}}\text{H}_2$ of axial **DAH** ligand, at range 8.63–7.93 ppm assigned to the $\text{Ar}-\underline{\text{C}}\text{H}$ of axial 4,4'-bpy ligand and at range 4.42–4.28 ppm assigned to the $\text{O}-\underline{\text{C}}\text{H}$, at range 4.22–4.16 ppm assigned to the $\text{O}-\underline{\text{C}}\text{H}_2$ and at range 2.62–0.86 ppm assigned to the $\underline{\text{N}}\text{H}_2$ and $\text{Aliph}-\underline{\text{C}}\text{H}_2$ of axial **TUPA** ligand, respectively. Besides, ^{13}C NMR resonance of axial-bridged ligands were detected at between 31.70 and 31.12 ppm assigned to $-\underline{\text{C}}\text{H}_2$ of axial **DAH** ligand, at

between 154.99 and 126.08 ppm assigned to *ortho*, *para* or *meta* $-\underline{\text{C}}$ of axial 4,4'-bpy ligand, and at between 102.39 and 21.01 ppm assigned to carbon resonance of axial **TUPA** ligand, respectively.

The LC–MS spectra for the dioxime (**L₁H₂**) and (**L₂H₂**) ligands and their dicobaloxime/organodicobaloxime (**1–12**) complexes were investigated. The Mass (LC–MS) spectral data of all compounds (ligands and complexes) supported the proposed structures due to the molecular ion peaks consistent with the molecular weight of the compounds. The designated results for peak positions and the isotopic distributions are given in the experimental part (Kilic et al. 2013b; Ruchi 2013). The values are in the range ~ 18 – $11 \Omega^{-1} \text{cm}^2 \text{mol}^{-1}$ in DMF), suggesting a non-electrolytic nature for the dicobaloxime/organodicobaloxime (**1–12**) complexes, and there is no counter ion present outside their coordination sphere. The measurements of magnetic moments of the dicobaloxime/organodicobaloxime (**1–12**) complexes were performed at 25 °C and in the solid state. These magnetic values show that the dicobaloxime/organodicobaloxime (**1–12**) complexes are diamagnetic form and the low-spin ($S = 0$) octahedral d^6 -systems due to the complete spin pairing as expected. Also, these magnetic results indicate that the cobalt center of cobaloximes is in the +3 oxidation state.

Electrochemical properties

Redox properties of the dicobaloxime and organodicobaloxime (**1–12**) complexes were studied on a glassy carbon electrode in DMSO containing 0.1 M $n\text{-Bu}_4\text{NClO}_4$ as the supporting electrolyte (Figs. 7, 8, 9, 10, 11). Table 1 summarizes the electrode potentials for the dicobaloxime and organodicobaloxime (**1–12**) complexes in DMSO. The cyclic voltammograms of the dicobaloxime (**1–6**) and organodicobaloxime (**7–12**) complexes is not well resolved

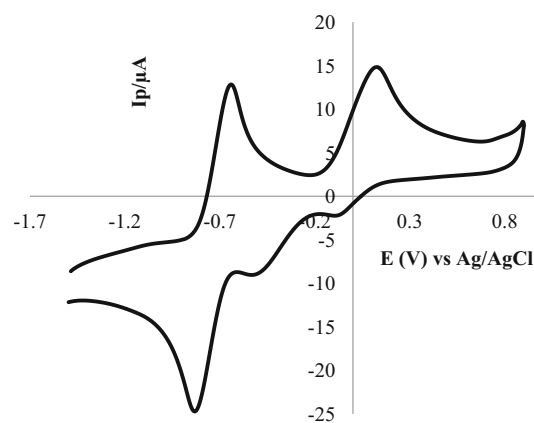


Fig. 7 A cyclic voltammogram of cobaloxime (**3**) complex in DMSO containing 0.1 M $n\text{-Bu}_4\text{NClO}_4$ as supporting electrolyte. Scan rate 100 mV/s

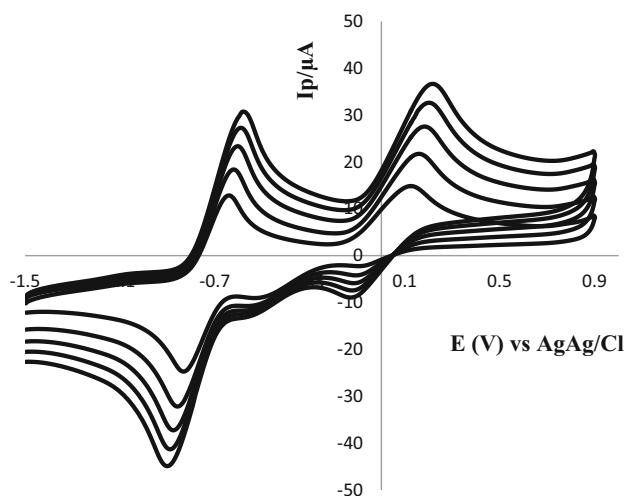


Fig. 8 Cyclic voltammogram of cobaloxime (**3**) complex in DMSO containing 0.1 M $n\text{-Bu}_4\text{NClO}_4$ as supporting electrolyte. Scan rates increasing from 100 to 500 mV/s

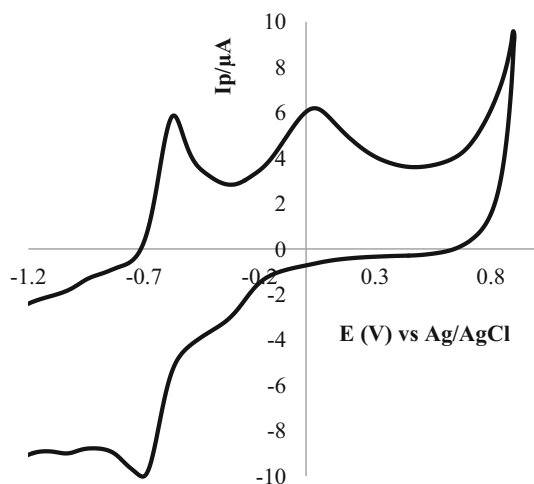


Fig. 9 A cyclic voltammogram of cobaloxime (**4**) complex in DMSO containing 0.1 M $n\text{-Bu}_4\text{NClO}_4$ as supporting electrolyte. Scan rate 100 mV/s

that probably the change in coordination number of cobalt center during reduction and oxidation process (Dutta and Gupta 2011). Among them, dicobaloxime (**1–6**) species give a better cyclic voltammogram as compared to its organodicobaloxime derivatives (**7–12**). Cyclic waves of the dicobaloxime (**3**) complex exhibits a quasi-reversible wave versus an Ag/AgCl which can be assigned to Co(III)/Co(II) couples. As shown in Fig. 7, the dicobaloxime (**3**) complex showed an oxidation peak at $E_{pa} = -0.647$ V with a corresponding reduction peak at $E_{pc} = -0.831$ V. The peak separation for this couple (ΔE_p) is 184 mV. The most significant feature of the formation Co(III)/Co(II) redox couple is the one-electron transfer via electrochemical process. The difference between anodic and cathodic

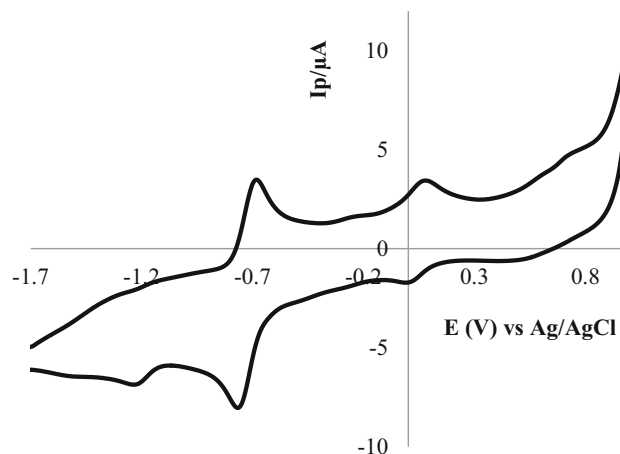


Fig. 10 A cyclic voltammogram of cobaloxime (**5**) complex in DMSO containing 0.1 M $n\text{-Bu}_4\text{NClO}_4$ as supporting electrolyte. Scan rate 100 mV/s

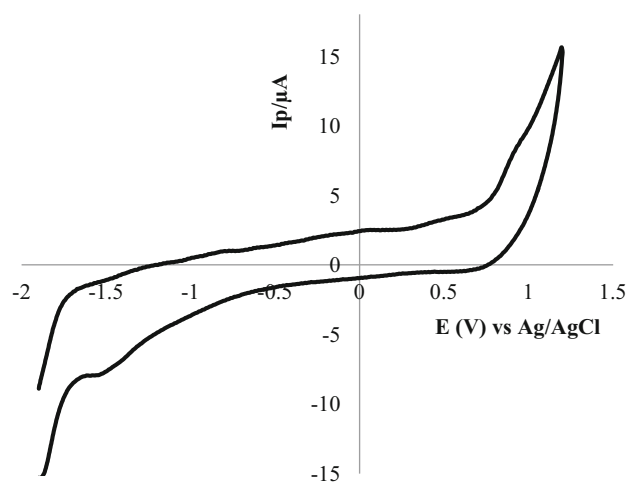


Fig. 11 A cyclic voltammogram of cobaloxime (**6**) complex in DMSO containing 0.1 M $n\text{-Bu}_4\text{NClO}_4$ as supporting electrolyte. Scan rate 100 mV/s

wave potentials can provide a rough evaluation of the degree of the reversibility of one-electron transfer process. The evaluation of cyclic voltammetric data with the scan rate varying 100–500 mV/s gives the evidence for a quasi-reversible one electron oxidation (Fig. 8). The ratio of reduction to oxidation wave height was less than one. However, the wave current increases with the increase of the square root of the scan rate. The $I_p/v^{1/2}$ value is almost constant for all scan rates. This establishes the electrode process as diffusion controlled (Bard and Faulkner 2001). The separation in wave potentials increases at higher scan rates. These characteristic features are consistent with the quasi-reversibility of Co(III)/Co(II) redox couple. Since the molecule is symmetrical both the cobalt centers behave similarly. This might be due to electron delocalization

between two cobalt centers by a substantial overlap of cobalt and axial ligand orbitals. The dicobaloxime (**3**) complex also shows another quasi-reversible redox wave ($E_{pa} = 0.116$ V and $E_{pc} = -0.079$ V) followed by an irreversible reduction peak at -0.501 V corresponding to the ligand moiety of the complex. The cyclic voltammogram of the dicobaloxime (**4**) complex (Fig. 9) shows an oxidation peak at $E_{pa} = -0.581$ V with a corresponding reduction peak at $E_{pc} = -0.706$ V which can be ascribed to Co(III)/Co(II) couples. The peak separation for this couple (ΔE_p) is 125 mV. The dicobaloxime (**4**) complex also shows one irreversible oxidation peak at $E_{pa} = 0.028$ V and one reduction peak at $E_{pc} = -0.347$ V corresponding to the ligand moiety of the complex. The dicobaloxime (**5**) complex exhibits an oxidation peak at $E_{pa} = -0.689$ V with a corresponding reduction peak at $E_{pc} = -0.762$ V which can be ascribed to Co(III)/Co(II) couples (Fig. 10). However, the irreversible reduction peak at -1.146 V may be ascribed to the formation of Co(I) species. The rest of oxidation and reduction peaks are possibly due to the oxime moiety of the complex. The dicobaloxime (**6**) complex exhibits only one oxidation peak at 0.903 V corresponding to the oxidation of ligand moiety and one reduction peak at -1.534 V corresponding to the formation of Co(I) as shown in Fig. 11. Cyclic voltammograms of the organodicobaloximes were poor. This is possibly due to the enhanced σ donation by R groups in the organocobaloximes which are substantially stabilized. In other words, in the organodicobaloximes redox processes are considerably cathodically shifted. Due to this, redox process is further cathodically shifted and therefore not observed in the accessible solvent window (Dutta et al. 2015).

Catalytic properties

The chemical fixation of CO₂ to synthesize useful chemicals in the presence of 0.1% dicobaloximes or organodicobaloximes (**1–12**) complexes was preferred as a model reaction for testing and the results are given in the Table 2. The cycloaddition of CO₂ and various epoxides catalyzed by dicobaloxime (**1–6**) and organodicobaloxime (**7–12**) complexes was investigated under adopted reaction

conditions. The catalytic tests were performed at optimized conditions, which were defined in our last studies (Kilic et al. 2013b; Ulusoy et al. 2011a, b). The dicobaloxime and organodicobaloxime compounds (**1–12**) showed good catalytic activity and selectivity for the transformation of CO₂ into cyclic carbonates using epoxide derivatives and presence of DMAP (4-dimethylamino pyridine) as Lewis base. Among the cobaloxime complexes, the organodicobaloxime (**10**) complex showed good catalytic activity and selectivity for the coupling of CO₂ and epichlorohydrin in the presence of DMAP as co-catalysts. (Table 2, entries 1–12). In this catalytic system, regarding reaction mechanism one Co(III) center was proposed to serve as Lewis acid for epoxide activation and another as a counterion for the nucleophile. In other words, for the understanding of reaction mechanism, the amine-based co-catalyst is necessary for the reaction in several different ways (first, DMAP acts as a Lewis base to attack the sterically less hindered carbon atom to open the epoxide ring, while the role of Co(III) is of a Lewis acid and activates the epoxide upon binding, and the generated oxyanion species then react with CO₂ to give the cyclic carbonate, and the cycle goes on) (Kilic et al. 2016). Here, two structurally different types of cobaloxime compounds were investigated. Type one is the dicobaloximes (**1–6**) and the other is the organometallic forms of cobalt (**7–12**) complexes (called organodicobaloxime). The organodicobaloxime (**10**) complex bearing Ph-CH₂- substituent to metal center indicated the best catalytic performance (Table 2) with epichlorohydrin as substrate. The main reason for the better catalytic efficiencies of the organodicobaloxime (**10**) complex may be the reaction media, where the differences between compounds, substrates and the purity of CO₂ could play a role. However, the high conversion was attributed to good diffusion and high miscibility of epichlorohydrin in CO₂ under studies conditions. Consequently, the organodicobaloxime (**10**) showed high conversion (78.0%) and selectivity (98%) (entry 10) compared to the other cobaloxime complexes, which may be attributed to the more Lewis acidic octahedral Co(III) centers in organodicobaloxime (**7–12**) complexes due to the presence of a benzyl group connecting instead of an electron-withdrawing

Table 1 Voltammetric data for cobaloximes (**3–6**) complexes

Complex	Metal centered			Ligand based oxidation/reduction			
	E_{pa} (V)	E_{pc} (V)	(ΔE_p) (mV)	E_{pc} (V)	E_{pa} (V)	E_{pc} (V)	E_{pc} (V)
3	-0.647	-0.831	184		0.116	-0.079	-0.501
4	-0.581	-0.706	125		0.028	-0.347	
5	-0.689	-0.762	73	-1.146	-		
6				-1.534	0.903		

Supporting electrolyte = 0.1 M n-Bu₄ClO₄, scan rate = 100 mV/s

Table 2 Synthesis of ECHC [4-(chloromethyl)-1,3-dioxolan-2-one] from ECH [2-(chloromethyl)oxirane] and CO₂ catalyzed by cobaloxime

Entry (%)	Cat.	Conversion ^a (%)	Selectivity ^a	TON ^b	TOF ^c (h ⁻¹)
1	1	61	99	606	303
2	2	59	98	593	297
3	3	44	98	443	222
4	4	65	98	653	327
5	5	56	98	556	278
6	6	60	99	595	298
7	7	68	99	682	341
8	8	53	98	530	265
9	9	59	98	588	294
10	10	78	98	780	390
11	11	62	99	617	309
12	12	62	98	618	309

^a Conversion and selectivity of epichlorohydrin to corresponding Epichlorohydrin carbonate were determined by GC

^b Moles of cyclic carbonate produced per mole of catalyst

^c The rate is expressed in terms of the turnover frequency {TOF [mol of product (mol of catalyst h⁻¹)] = turnovers/h}

chlorine atom as axial ligand. However, we have carried out the blank reaction without catalyst. To ascertain the activity of DMAP alone in this reaction under the given conditions the catalytic blank-run without Co(III) catalyst was done and found to be 5% conversion.

We have executed similar catalytic tests changing the reaction time, reaction temperature, ambient pressure, various base and different epoxide to find the better reaction conditions. In the beginning, the studies of cyclohexene oxide (CHO), styrene oxide (SO), epichlorohydrin (ECH), propylene oxide (PO), and 1, 2-epoxybutane (EB) as substrates with CO₂ to synthesize the corresponding cyclic carbonates were investigated. As shown in Fig. 12, among them epichlorohydrin was found to be the most reactive epoxide compared to the other epoxides whose propylene epoxide exhibited the lowest activity. It was found that epichlorohydrin (ECH) was the most reactive one (due to the fact that the electron-withdrawing chloromethyl group of epichlorohydrin could assist the breaking of C–O bond of the epoxide, thus favouring the subsequent CO₂ addition to the opened epoxy), while cyclohexene oxide (CHO) exhibited the lowest activity. Also, the internal epoxide, cyclohexene oxide is converted to the corresponding cyclic carbonate with low yield presumably due to the high steric hindrance (Bai et al. 2013).

The results of optimization conditions such as reaction temperature, epoxide, time and CO₂ pressure were very similar to those of homogeneous and heterogeneous systems previously reported (Ulusoy et al. 2009; Kilic et al. 2010). In addition, the DMAP, KOH, Na₂CO₃, Na₂SO₄ and Cs₂CO₃ were tested for comparison of base effect. The necessity of a base was observed as shown in Fig. 13. Interestingly, the use of Cs₂CO₃ resulted in a yield of 19%, and the yield remarkably increased 78% when DMAP was used as the base (Fig. 13) in high selectivity (Ulusoy et al. 2011a, b). These results showed that organic base showed a better activity than from the inorganic bases.

It is generally adopted that reaction parameters such as reaction time, temperature and initial CO₂ pressure have a significant effect on the catalytic activity of conversion of ECH to its related cyclic organic carbonate (Fig. 14) using the organodicobaloxime (**10**) as a catalyst. As shown in Fig. 14a, when the temperature rises from 75 to 125 °C, [4-(chloromethyl)-1,3-dioxolan-2-one] (ECHC) yield increased sharply from 20 to 96%. These results show that the temperature rise has an apparent positive effect on the transformation of ECH to its related cyclic organic carbonate. However, the temperature rises from 125 to 150 °C, ECHC yield slight decreased from 96 to 93% (Fig. 14a). Therefore, from a practical viewpoint, the

Fig. 12 The conversion of various epoxides to corresponding cyclic carbonates at the same catalytic conditions with organocobaloxime (**10**) as catalyst

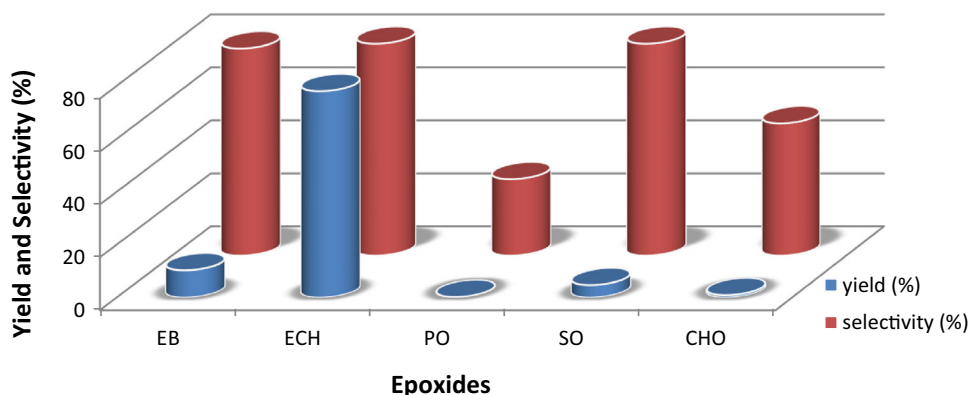
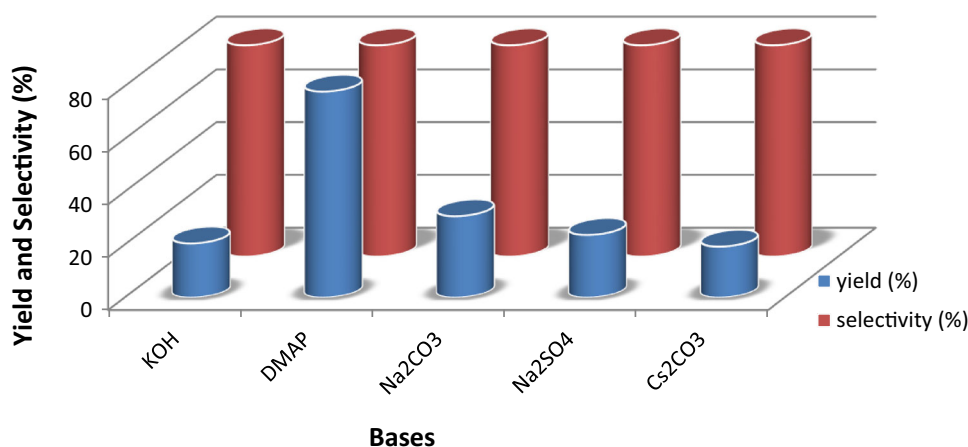


Fig. 13 Conversion and selectivity of 2-(chloromethyl) oxirane as effect the transformation of base at the same catalytic conditions with organocobaloxime (**10**) as catalyst



optimal reaction temperature has been accepted as 100 °C for adopted catalytic conditions. As shown in Fig. 14b, in the low-pressure range (0.5–1.6 MPa), there is rise of [4-(chloromethyl)-1,3-dioxolan-2-one] (ECHC) yield (from 70 to 78%) with increase of initial CO₂ pressure, but further rise of pressure to 2.5 MPa results in moderate decrease of ECHC yield. The reason for these results, a higher initial CO₂ pressure can effectively increase the solubility of CO₂ in epichlorohydrin (ECH), permitting the reaction equilibrium to shift toward carbonate formation. However, when the initial CO₂ pressure reached 2.5 MPa, this high CO₂ pressure may have retarded the interaction between ECH and catalysts, resulting in a decrease in the transformation of ECH to its related cyclic organic carbonate. A similar effect was reported in our previous paper (Ulusoy et al. 2009). As shown in Fig. 14c, the cycloaddition reaction proceeds rapidly within the first 2 h, reaching an [4-(chloromethyl)-1,3-dioxolan-2-one] (ECHC) yield of 78%. With the increase of reaction time from 0.5 h to 4 h, ECHC yield increased sharply from 40% to 89%.

Conclusion

In summary, the different substituted axial diamine-bridged dicobaloxime and organodicobaloximes have been synthesized for the first time. These Co(III) complexes (**1–12**) were successfully characterized by various spectroscopic methods such as NMR (¹H and ¹³C) spectroscopy, UV–Visible spectroscopy, FT-IR spectroscopy, Mass spectroscopy, molar conductivity analysis, melting point, and magnetic susceptibility experiments with elemental analysis and cyclic voltammetry (CV). The cyclic voltammograms of the organodicobaloximes were poor. This is possibly due to the enhanced σ donation by R groups in the organodicobaloximes which are substantially stabilized. These obtained complexes also were used for conversion of carbon dioxide to cyclic carbonates as homogeneous catalysts under mild conditions. The best active catalyst organodicobaloxime (**10**) complex was not effective in epoxides (EB, SO, PO and CHO). Whereas using the epichlorohydrin (ECH) as epoxide, good conversion and selectivity were achieved at the same catalytic conditions.

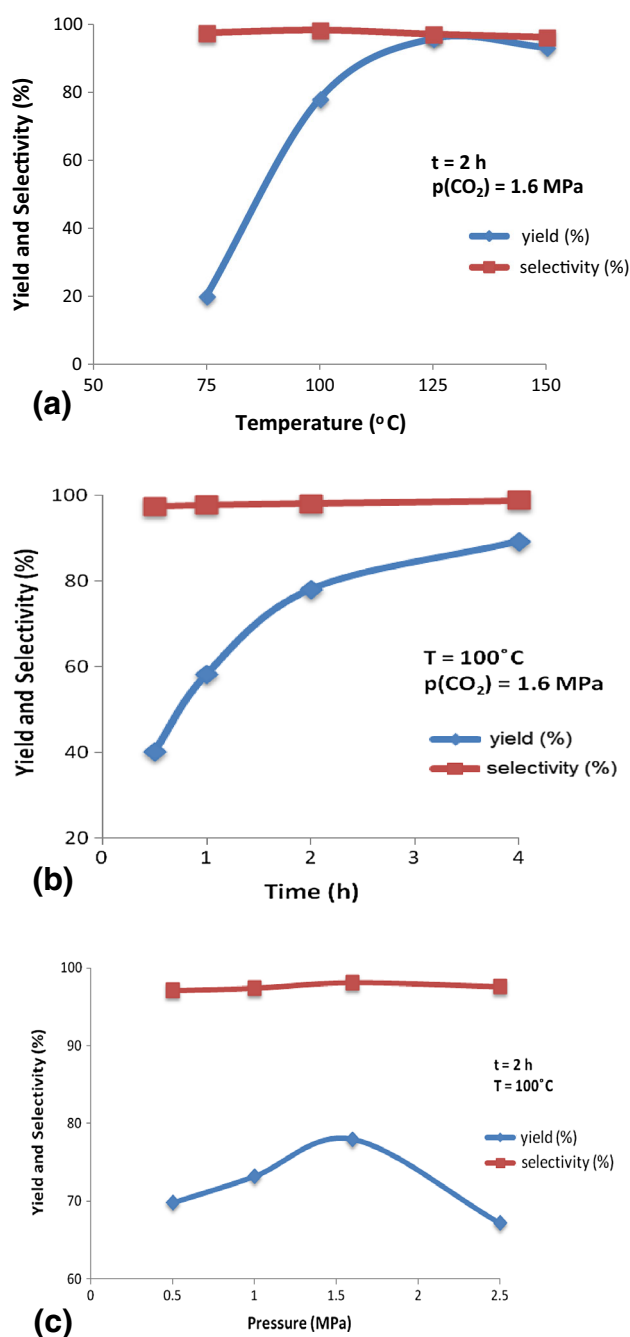


Fig. 14 Conversion and selectivity of epichlorohydrin as a function of temperature (a), pressure (b) and time (c) with complex organocobaloxime (10) as catalyst

The organodnicobaloxime (10) complex shows that high conversion (78.0%) and selectivity (98%) for the conversion of CO_2 into cyclic carbonates when DMAP was used as co-catalyst.

Acknowledgement We acknowledge the TUBITAK (Technological and Scientific Research Council of Turkey) for support of this research (Project No: 111T944).

References

- Alici O, Karatas I (2016) Novel liquid crystal aldoximes and aldoxime ethers: synthesis, characterization and liquid crystal behavior. *J Mol Liquids* 221:1243–1248. doi:10.1016/j.molliq.2015.04.016
- Al-Qaisi F, Genjang N, Nieger M, Repo T (2016) Synthesis, structure and catalytic activity of bis(phenoxyiminato)iron(III) complexes in coupling reaction of CO_2 and epoxides. *Inorg Chim Acta* 442:81–85. doi:10.1016/j.ica.2015.11.023
- Anastas PT, Lankey RL (2000) Life cycle assessment and green chemistry: the yin and yang of industrial ecology. *Green Chem* 2:289–295. doi:10.1039/B005650M
- Artero V, Chavarot-Kerlidou M, Fontecave M (2011) Splitting water with cobalt. *Angew Chem Int Ed* 50:7238–7266. doi:10.1002/anie.201007987
- Bai D, Nian G, Wang Z (2013) Titanocene dichloride/KI: an efficient catalytic system for synthesis of cyclic carbonates from epoxides and CO_2 . *Appl Organometal Chem* 27:184–187. doi:10.1002/aoc.2967
- Balzani V, Juris A, Venturi M, Campagna S, Serroni S (1996) Luminescent and redox-active polynuclear transition metal complexes. *Chem Rev* 96:759–834. doi:10.1021/cr941154y
- Bard AJ, Faulkner LR (2001) *Electrochemical methods: fundamentals and applications*, 2nd edn. Wiley, New York
- Brown KL (1972) Mechanism of base-catalyzed methane formation from methyl(aquo)cobaloxime. *J Am Chem Soc* 94:388–393
- Castro-Gomez F, Salassa G, Kleij AW, Bo C (2013) A DFT study on the mechanism of the cycloaddition reaction of CO_2 to epoxides catalyzed by Zn(Salphen) complexes. *Chem Eur J* 19:6289–6298. doi:10.1002/chem.201203985
- Cini R, Moore SJ, Marzilli LG (1998) Strong trans influence methoxymethyl ligand in B_{12} cobaloxime and imine/oxime model complexes: structural, spectroscopic, and molecular mechanics investigations. *Inorg Chem* 37:6890–6896. doi:10.1021/ic980666i
- Connolly P, Espenson JH (1986) Cobalt-catalyzed evolution of molecular hydrogen. *Inorg Chem* 25:2684–2688. doi:10.1021/ic00236a006
- Cuesta-Aluja L, Campos-Carrasco A, Castilla J, Reguero M, Masdeu-Bultó AM, Aghmiz A (2016) Highly active and selective Zn(II)-NN'O Schiff base catalysts for the cycloaddition of CO_2 to epoxides. *J CO₂ Utiliz* 14:10–22. doi:10.1016/j.jcou.2016.01.002
- Darensbourg DJ, Holtcamp MW (1996) Catalysts for the reactions of epoxides and carbon dioxide. *Coord Chem Rev* 153:155–174. doi:10.1016/0010-8545(95)01232-X
- Dempsey JL, Brunschwig BS, Winkler JR, Gray HB (2009) Hydrogen evolution catalyzed by cobaloximes. *Acc Chem Res* 42:1995–2004. doi:10.1021/ar900253e
- Dreos R, Randaccio L, Seiga P, Tavagnacco C, Zangrando E (2010) Guest driven self-assembly of a rectangular box from methylaquacobaloxime and 4,4'-biphenyldiboronic acid. *Inorg Chim Acta* 363:2113–2124. doi:10.1016/j.ica.2010.02.023
- Du P, Knowles K, Eisenberg R (2008) A homogeneous system for the photogeneration of hydrogen from water based on a platinum(II) terpyridyl acetylide chromophore and a molecular cobalt catalyst. *J Am Chem Soc* 130:12576–12577. doi:10.1021/ja804650g
- Dutta G, Gupta BD (2011) Cobaloximes with mixed dioximes having C and S side chains: synthesis, structure and reactivity. *J Organomet Chem* 696:2693–2701. doi:10.1016/j.jorganchem.2011.02.033
- Dutta G, Mandal D, Gupta BD (2012) Pyrazine bridged dicobaloximes with bis(thiophenyl)glyoxime and their molecular oxygen

- insertion. *J Organomet Chem* 706–707:30–36. doi:[10.1016/j.jorganchem.2012.01.009](https://doi.org/10.1016/j.jorganchem.2012.01.009)
- Eckenhoff WT, McNamara WR, Du P, Eisenberg R (2013) Cobalt complexes as artificial hydrogenases for the reductive side of water splitting. *Biochimica Biophysica Acta* 1827:958–973. doi:[10.1016/j.bbabi.2013.05.003](https://doi.org/10.1016/j.bbabi.2013.05.003)
- Herlinger AW, Ramakrishna K (1985) Synthesis and characterization of neutral ligand-bridged binuclear dialkylcobalt(III) complexes. *Polyhedron* 4:551–561. doi:[10.1016/S0277-5387\(00\)86661-9](https://doi.org/10.1016/S0277-5387(00)86661-9)
- Kilic A, Ulusoy M, Durgun M, Tasci Z, Yilmaz I, Cetinkaya B (2010) Hetero- and homo-leptic Ru(II) catalyzed synthesis of cyclic carbonates from CO₂; Synthesis, spectroscopic characterization and electrochemical properties. *Appl Organomet Chem* 24:446–453. doi:[10.1002/aoc.1638](https://doi.org/10.1002/aoc.1638)
- Kilic A, Palali AA, Durgun M, Tasci Z, Ulusoy M (2013a) The coupling of carbon dioxide and epoxides by phenanthroline derivatives containing different Cu(II) complexes as catalyst. *Spectrochim Acta A* 113:432–438. doi:[10.1016/j.saa.2013.04.124](https://doi.org/10.1016/j.saa.2013.04.124)
- Kilic A, Palali AA, Durgun M, Tasci Z, Ulusoy M, Dagdevren M, Yilmaz I (2013b) Synthesis, characterization, electrochemical properties and conversions of carbon dioxide to cyclic carbonates mononuclear and multinuclear oxime complexes using as catalyst. *Inorg Chim Acta* 394:635–644. doi:[10.1016/j.ica.2012.09.020](https://doi.org/10.1016/j.ica.2012.09.020)
- Kilic A, Kilic MV, Ulusoy M, Durgun M, Aytar E, Dagdevren M, Yilmaz I (2014) Ketone synthesized cobaloxime/organocobaloxime catalysts for cyclic carbonate synthesis from CO₂ and epoxides: characterization and electrochemistry. *J Organomet Chem* 767:150–159. doi:[10.1016/j.jorganchem.2014.05.023](https://doi.org/10.1016/j.jorganchem.2014.05.023)
- Kilic A, Ulusoy M, Aytar E, Durgun M (2015) Mono/multinuclear cobaloxime and organocobaloxime-catalyzed conversion of CO₂ and epoxides to cyclic organic carbonates: synthesis and characterization. *J Ind Eng Chem* 24:98–106. doi:[10.1016/j.jiec.2014.09.015](https://doi.org/10.1016/j.jiec.2014.09.015)
- Kilic A, Akdag S, Aytar E, Durgun M, Ulusoy M (2016) Design, synthesis and characterization of novel dioxime ligand-based cobaloxime compounds for application in the coupling of CO₂ with epoxides. *New J Chem* 40:7901–7910. doi:[10.1039/c6nj01223j](https://doi.org/10.1039/c6nj01223j)
- Kumar S, Seidel RW (2013) Ligand-bridged bicobaloximes synthesized by ligand replacement: synthesis, structure and characterization. *Inorg Chem Commun* 27:1–4. doi:[10.1016/j.inoche.2012.10.019](https://doi.org/10.1016/j.inoche.2012.10.019)
- Lawrence MAW, Celestine MJ, Artis ET, Joseph LS, Esquivel DL, Ledbetter AJ, Cropek DM, Jarrett WL, Bayse CA, Brewer MI, Holder AA (2016) Computational, electrochemical, and spectroscopic studies of two mononuclear cobaloximes: the influence of an axial pyridine and solvent on the redox behaviour and evidence for pyridine coordination to cobalt(I) and cobalt(II) metal centres. *Dalton Trans* 45:10326–10342. doi:[10.1039/c6dt01583b](https://doi.org/10.1039/c6dt01583b)
- Lever ABP (1968) *Inorganic electronic spectroscopy*. Elsevier, Amsterdam
- Martinez J, Castro-Osma JA, Earlam A, Alonso-Moreno C, Otero A, Lara-Sanchez A, North M, Rodriguez-Dieguez A (2015) Synthesis of cyclic carbonates catalysed by aluminium heteroscorpionate complexes. *Chem Eur J* 21:9850–9862. doi:[10.1002/chem.201500790](https://doi.org/10.1002/chem.201500790)
- Mirra S, Strianese M, Pellicchia C, Bertolasi V, Monaco G, Milione S (2016) Influence of coordinated ligands in a series of inorganic cobaloximes. *Inorg Chim Acta* 444:202–208. doi:[10.1016/j.ica.2016.01.040](https://doi.org/10.1016/j.ica.2016.01.040)
- Moore EA and Janes R (2004) in *Metal-Ligand Bonding*, ed. E. W. Abel, RSC, ISBN: 978-0-85404-979-0
- Nayak SC, Das PK, Sahoo KK (2003) Synthesis and characterization of some cobalt(III) complexes containing heterocyclic nitrogen donor ligands. *Chem Pap* 57(2):91–96
- Niklas J, Mardis KL, Rakhimov RR, Mulfort KL, Tiede DM, Poluektov OG (2012) The hydrogen catalyst cobaloxime: a multifrequency EPR and DFT study of cobaloxime's electronic structure. *J Phys Chem B* 116:2943–2957. doi:[10.1021/jp209395n](https://doi.org/10.1021/jp209395n)
- Randaccio L (1999) Vitamin B₁₂ coenzyme models: perspectives on recent developments in the chemistry of the cobaloximes and related models. *Comments Inorg Chem* 21:327–376. doi:[10.1080/02603599908012011](https://doi.org/10.1080/02603599908012011)
- Razavet M, Artero V, Fontecave M (2005) Proton electroreduction catalyzed by cobaloximes: functional models for hydrogenases. *Inorg Chem* 44:4786–4795. doi:[10.1021/ic050167z](https://doi.org/10.1021/ic050167z)
- Roberts GE, Heuts JPA, Davis TP (2000) Direct observation of cobalt–carbon bond formation in the catalytic chain transfer polymerization of methyl acrylate using matrix-assisted laser desorption ionization time-of-flight mass spectrometry. *Macromolecules* 33:7765–7768. doi:[10.1021/ma0003506](https://doi.org/10.1021/ma0003506)
- Ruchi SC (2013) Synthesis, spectroscopic characterization, molecular modeling and antimicrobial activities of Mn(II), Co(II), Ni(II), Cu(II) complexes containing the tetradentate aza Schiff base ligand. *Spectrochim Acta A* 103:338–348. doi:[10.1016/j.saa.2012.10.065](https://doi.org/10.1016/j.saa.2012.10.065)
- Schrauzer GN, Kohnle J (1964) Coenzym B₁₂-modelle. *J Chem Ber* 97:3056–3064. doi:[10.1002/cber.19640971114](https://doi.org/10.1002/cber.19640971114)
- Stolzenberg AM, Workman SR, Gutshall JE, Jeffrey E, Petersen L, Akhmedov N (2007) Syntheses and characterization of organogroup 14 cobaloxime compounds. *Inorg Chem* 46:6744–6754. doi:[10.1021/ic070251+](https://doi.org/10.1021/ic070251+)
- Ulusoy M, Cetinkaya E, Cetinkaya B (2009) Conversion of carbon dioxide to cyclic carbonates using diimine Ru(II) complexes as catalysts. *Appl Organomet Chem* 23:68–74. doi:[10.1002/aoc.1473](https://doi.org/10.1002/aoc.1473)
- Ulusoy M, Kilic A, Durgun M, Tasci Z, Cetinkaya B (2011a) Silicon containing new salicylaldimine Pd(II) and Co(II) metal complexes as efficient catalysts in transformation of carbon dioxide (CO₂) to cyclic carbonates. *J Organometal Chem* 696:1372–1379. doi:[10.1016/j.jorganchem.2011.01.005](https://doi.org/10.1016/j.jorganchem.2011.01.005)
- Ulusoy M, Sahin O, Kilic A, Buyukgungor O (2011b) Multinuclear Cu(II) Schiff base complex as efficient catalyst for the chemical coupling of CO₂ and epoxides: synthesis, X-ray structural characterization and catalytic activity. *Cat Lett* 141:717–725. doi:[10.1007/s10562-010-0529-3](https://doi.org/10.1007/s10562-010-0529-3)
- Wang M, Han K, Zhang S, Sun L (2015) Integration of organometallic complexes with semiconductors and other nanomaterials for photocatalytic H₂ production. *Coord Chem Rev* 287:1–14. doi:[10.1016/j.ccr.2014.12.005](https://doi.org/10.1016/j.ccr.2014.12.005)
- Wani MY, Kumar S, Arranja CT, Dias CMF, Sobral AJFN (2016) Cycloaddition of CO₂ to epoxides using di-nuclear transition metal complexes as catalysts. *New J Chem* 40:4974–4980. doi:[10.1039/c5nj03198b](https://doi.org/10.1039/c5nj03198b)
- Xiang M, Meng QY, Li JX, Zheng YW, Ye C, Li ZJ, Chen B, Tung CH, Wu LZ (2015) Activation of C–H bonds through oxidant-free photoredox catalysis: cross-coupling hydrogen-evolution transformation of isochromans and β-keto esters. *Chem Eur J* 21:18080–18084. doi:[10.1002/chem.201503361](https://doi.org/10.1002/chem.201503361)
- Yamuna R, Sarath S, Kubandiran K, Umadevi M, Chakkaravarthi G (2016) Synthesis, characterization and thermal studies of 1,3-bis(4-pyridyl)propane bridged dicobaloximes. *J Organomet Chem* 811:40–47. doi:[10.1016/j.jorganchem.2016.03.015](https://doi.org/10.1016/j.jorganchem.2016.03.015)
- Yilmaz I, Kilic A, Yalcinkaya H (2008) Synthesis, characterization, fluorescence and redox features of new *vic*-dioxime ligand bearing pyrene and its metal complexes. *Chem Papers* 62(4):398–403. doi:[10.2478/s11696-008-0046-7](https://doi.org/10.2478/s11696-008-0046-7)